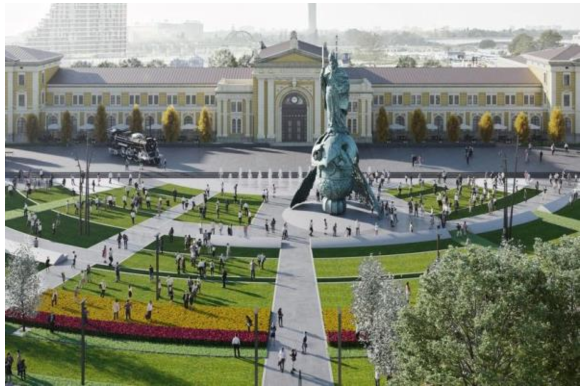

Mathematical Institute
of the Serbian Academy of
Sciences and Arts

Physics of Life
Biological Oscillators

Andjelka N. Hedrih

Department of Mechanics, Mathematical Institute of Serbian Academy of Science and Arts,
Kneza Mihaila 36, 11 000 Belgrade, Serbia
e-mail: handjelka@turing.mi.sanu.ac.rs ; handjeka@gmail.com

Mathematical modelling of biological systems

Some problems:

- Multidisciplinarity *(biology, medicine, theory of oscillations, theory of elasticity, rheology, non-linear dynamics)
- Complexity of biological systems- simplification
- appropriate approach
- The principle of phenomenological mapping
- Accuracy of the model-how to verify the theoretical model
- Limitations of the model

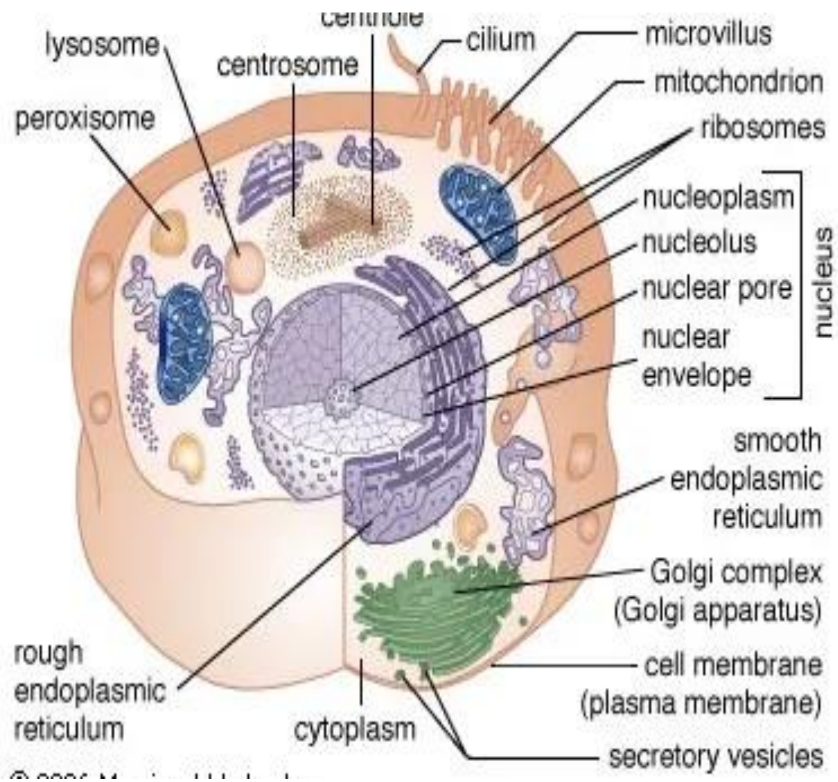

Taken from https://www.britannica.com/science/cell-biology

Adequacy of the model

- High-cell density tumour compartments were created using a custom-designed fabrication system and
- standardized oligomeric type I collagen to define and modulate ECM physical properties.

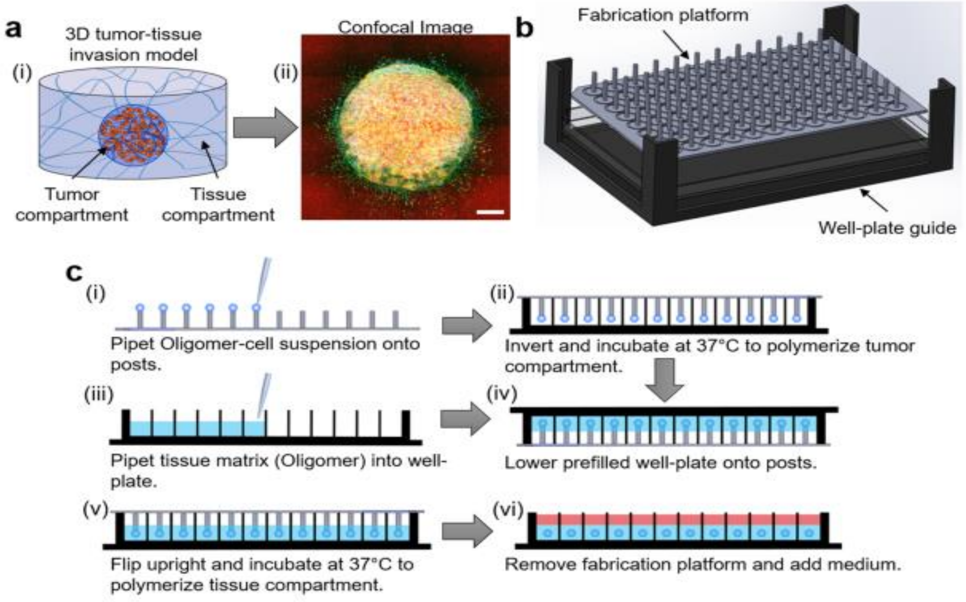

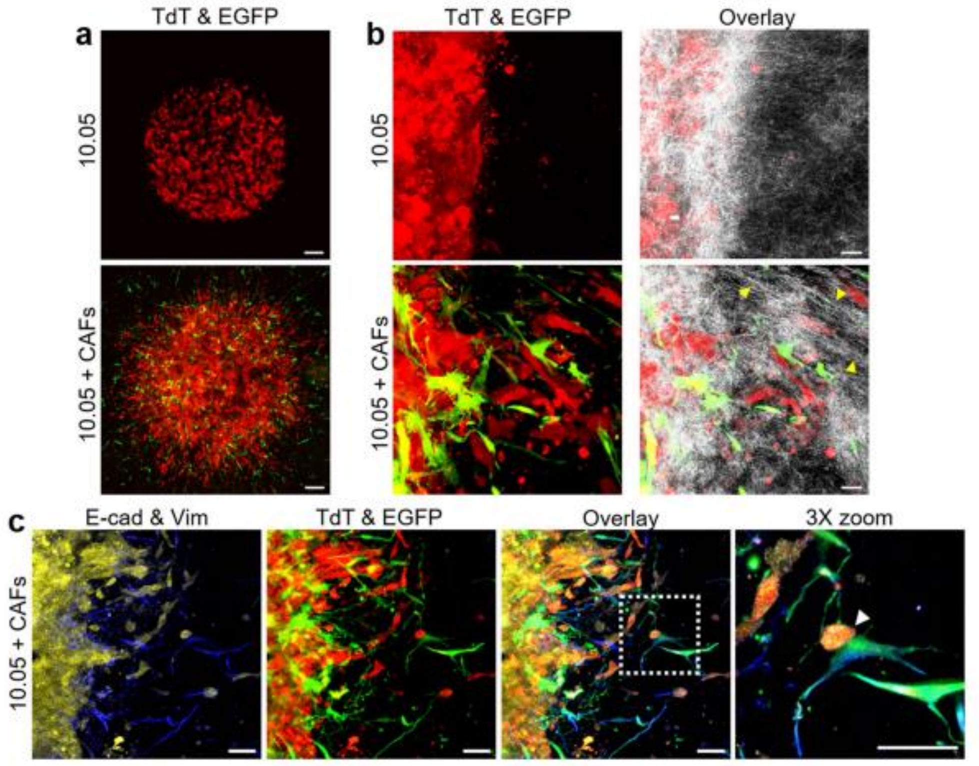

Figure 5. CAFs enhance invasiveness of patient-derived PDAC cells. The 3D tumor-tissue invasion model was prepared with 200 Pa Oligomer for both the tumor and surrounding tissue compartments. Tumor compartments were created with 10.05 alone or 10.05 + CAFS (at 1:1 ratio) at 1×10^7 cells/mL in Oligomer and cultured 4 days. (**a**) Images represent nine fields of view, each of which is a maximum projection of a 400 µm confocal z-stack. Red = tumor cells (TdT) and green = CAFs (EGFP). Scale bars = 200 µm. (**b**) Images represent maximum projections of 10 µm confocal z-stacks from cryosectioned constructs. Confocal reflection microscopy (white) was used to visualize matrix microstructure. Yellow arrowheads denote matrix alignment and remodeling; scale bars = 20 µm. (**c**) Images represent maximum projections of a 20 µm confocal z-stacks of cryosectioned constructs stained for E-cadherin (yellow) and vimentin (blue). Final panel represents a 3X zoom of boxed region in overlay panel. White arrowhead denotes direct interaction between tumor cell and CAF; scale bars = 50 µm.

Taken from SCientifiC RePorTS | (2018) 8:13039 | DOI:10.1038/s41598-018-31138-6

Adequacy of the model

- Tumor-on-a-chip

photolithography and 3D bioprinting

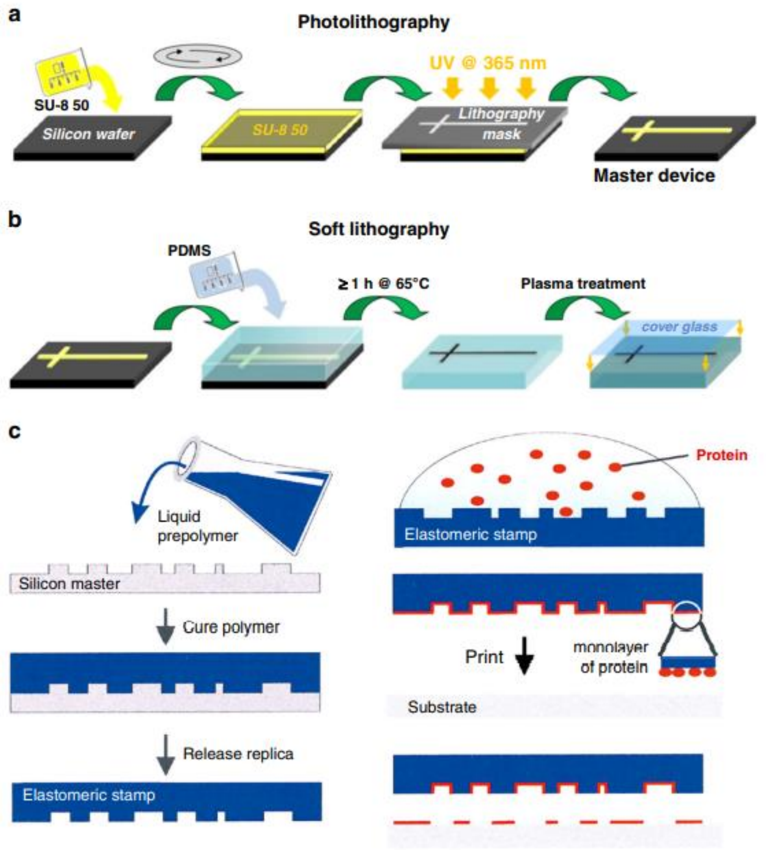

Fig. 2 Microfabrication techniques for tumor-on-a-chip. a, b Use of photolithography and soft lithography to fabricate a simple PDMS microfluidic culture device, conformally sealing it to a flat glass substrate. Adapted with permission[136]. Copyright 2013, RSC. **c** Use of microcontact printing to generate a protein pattern for cell culture. Adapted with permission[144]. Copyright 2000, Wiley.

in cancer biology and anticancer therapy research?

Taken from Liu et al. Microsystems & Nanoengineering (2021) 7:50 Microsystems & Nanoengineering https://doi.org/10.1038/s41378-021-00277-8

3D bioprinting of different type of tissue

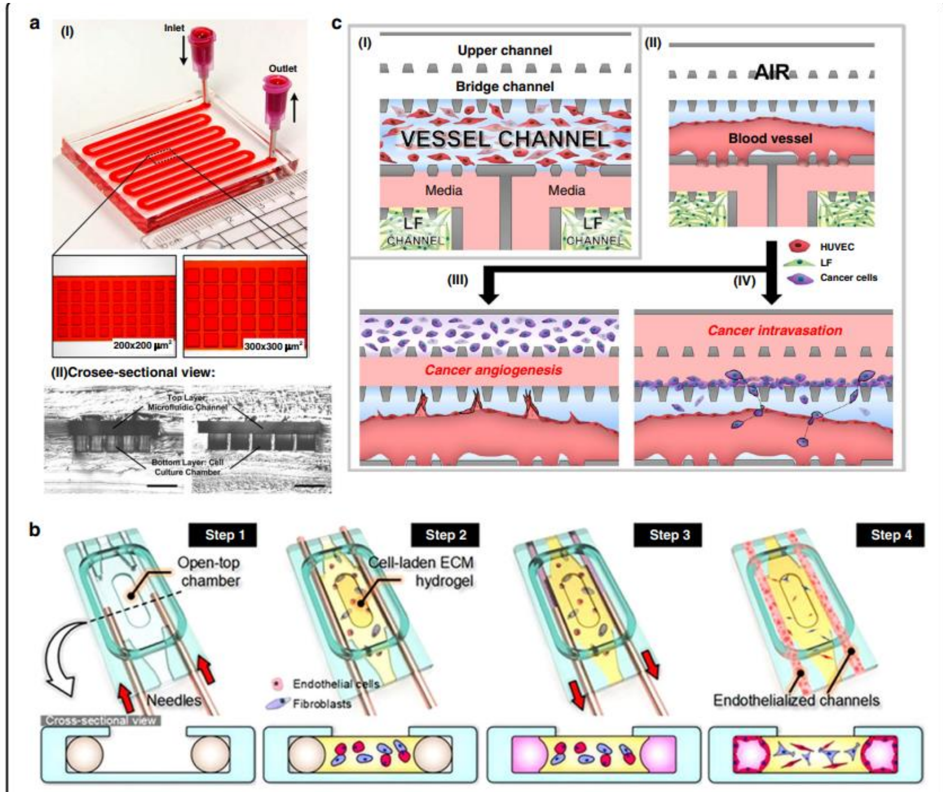

Fig. 4 Advanced tumor-on-a-chip models. a Microfluidic device for drug testing and flow cytometry analysis of tumor spheroids. I Two-layered microfluidic devices with different culture chamber geometries to prepare spheroids of different sizes for drug testing. II Microscopic cross-sectional views of microfluidic devices with different culture chamber geometries. Scale bar is 500 µm. Adapted with permission[178]. Copyright 2016, Springer Nature. **b** A microfluidic platform of perfusable microvascular beds to produce vascularized three-dimensional human microtissues. Adapted with permission[182]. Copyright 2016, Springer Nature. **c** A microfluidic metastasis chip platform for microvessel formation to analyze cancer angiogenesis and intravasation. I Schematic diagram of the microfluidic metastasis chip. II Microvessel formation. III Cancer angiogenesis. IV Cancer intravasation. Adapted with permission[183]. Copyright 2016, Springer Nature.

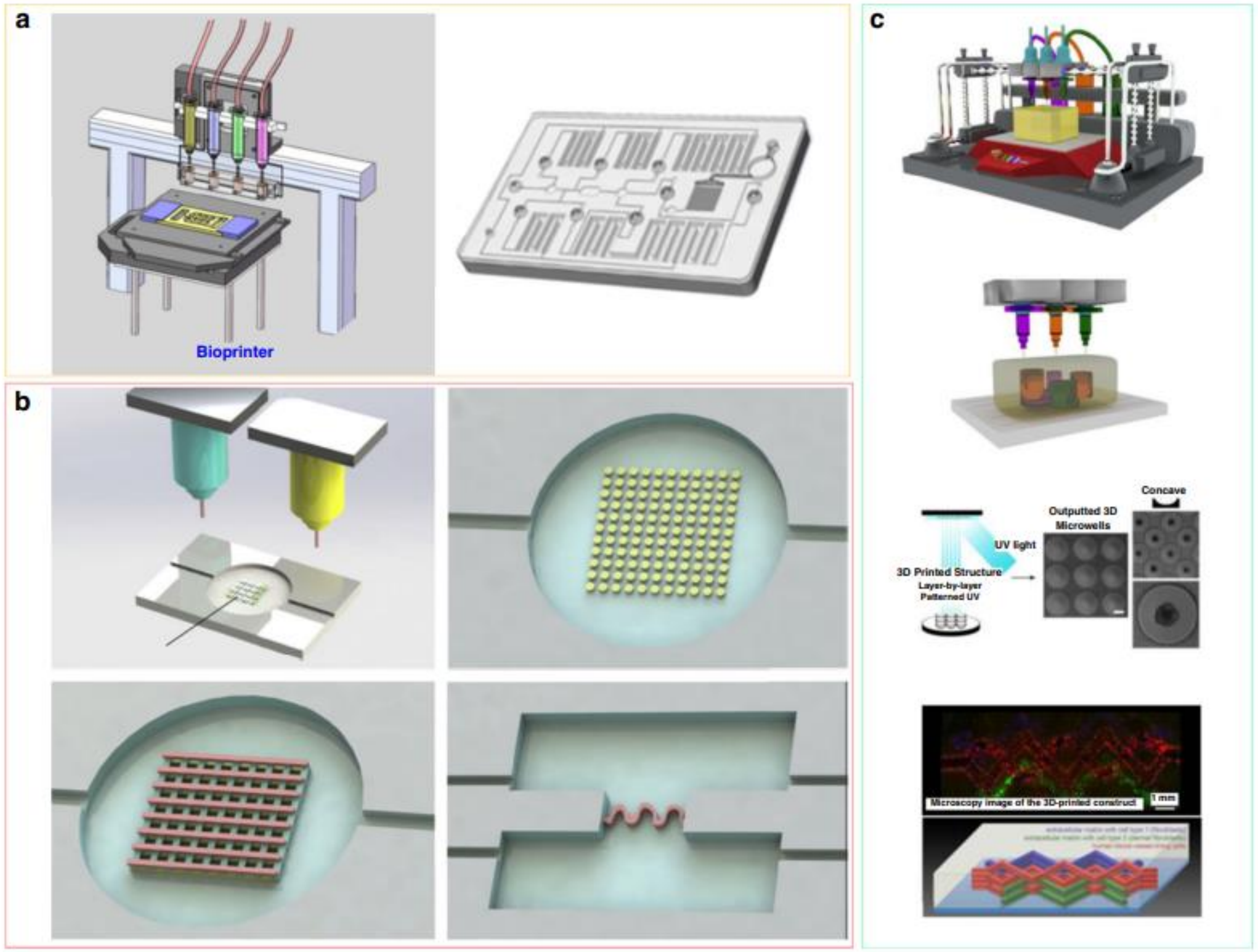

Fig. 3 Bioprinting technology for tumor-on-a-chip fabrication. a Using 3D bioprinting to create microfluidic chips for 2D/3D microtissue culture. Adapted with permission[130]. Copyright 2017, American Institute of Physics. **b** 3D bioprinting was used to produce different patterns and complex 3D microstructures to model the TME. Adapted with permission[158]. Copyright 2019, Elsevier. **c** Using 3D bioprinting to fabricate heterogeneous tissues: 3D microwells were constructed to facilitate spheroid formation and vascularized tissue models. Adapted with permission[159]. Copyright 2016, Whioce Publishing Pte. Ltd.

Adequacy of the model-application

Antitumor drug efficacy,
antiangiogenic drugs’ efficacy

Taken from Vincent Roy et al, Volume 2020, Article ID 6051210, 23 pages https://doi.org/10.1155/2020/6051210

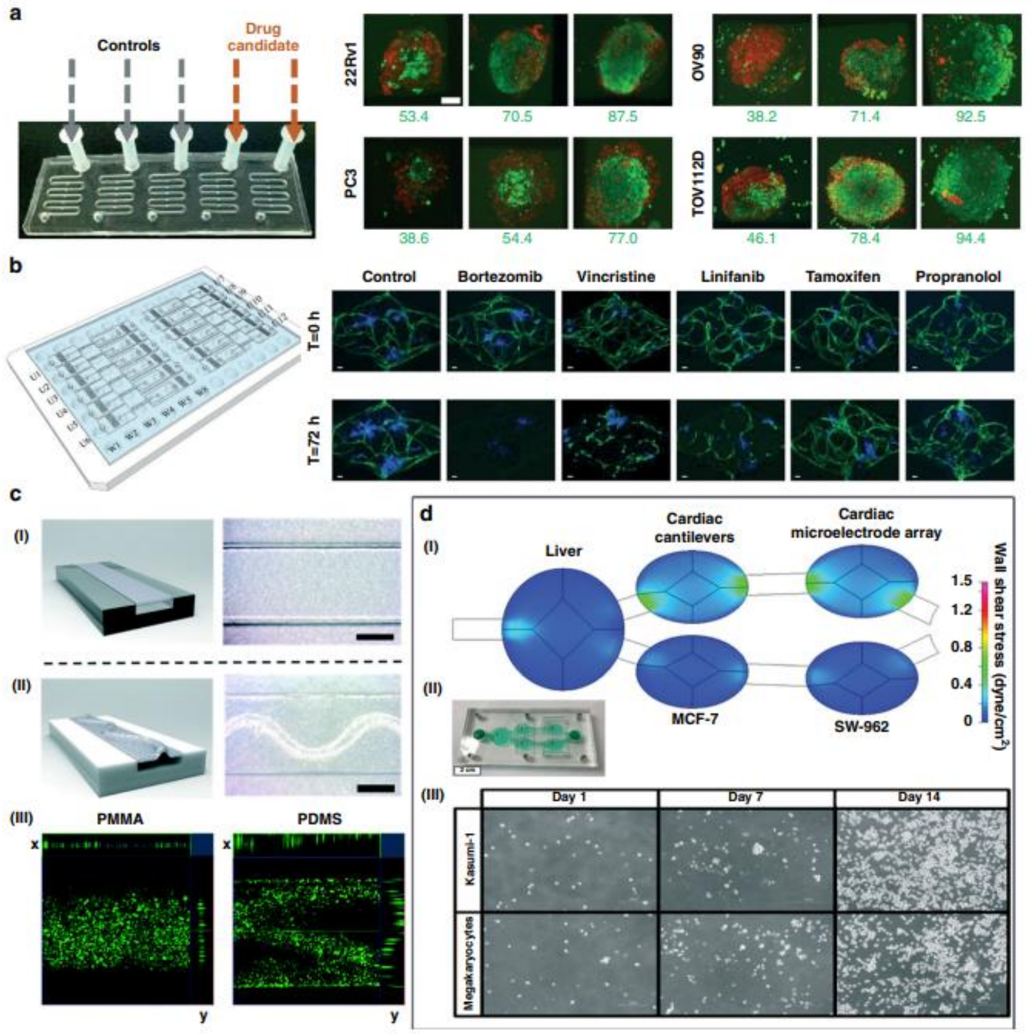

Fig. 8 Illustration of tumor-on-a-chip devices applied to drug screening. a The microdissected tumor/tissue samples (MDTs) were incubated in independent chambers of a microfluidics chip to assess one or several selected drug candidates. Some were treated with drugs, and the others were kept as nontreated controls. MDTs were labeled with viability dyes: CTG (live, green) and PI (dead, red). Adapted with permission[121]. Copyright 2016, The Royal Society of Chemistry. **b** A vascularized and perfused organ-on-a-chip platform for large-scale drug screening has been applied to some FDA-approved anticancer drug-blinded screenings, successfully identifying both antiangiogenesis and antitumor drugs. Adapted with permission[86]. Copyright 2017, The Royal Society of Chemistry. **c** Comparison diagram of the microfluidic chip models made by PMMA and PDMS. I The PMMA-PETE device with flat PETE membrane. II The PDMS-PETE device with wrinkled PETE membrane. III Confocal microscopic images of human lung adenocarcinoma cells cultured on PETE membrane in the PMMA and PDMS devices and stained with calcein. Adapted with permission[164]. Copyright 2019, The Royal Society of Chemistry. **d** The five-chamber reconfigurable multiorgan system platform used to evaluate the efficacy and off-target toxicity of anticancer drugs. I Computational fluid dynamics modeling. II Photograph of the multi-organ system. III Representative phase contrast images of Kasumi-1 and megakaryocytes growing inside the multi-organ system chamber on days in vitro (DIV) 1, 7, and 14. Adapted with permission[230].

meaningfulness of scientific results

Replicating results is crucial
Testing, validating, retesting

Fitting the data

- example

Sperm encapsulation

$CaCl_2$

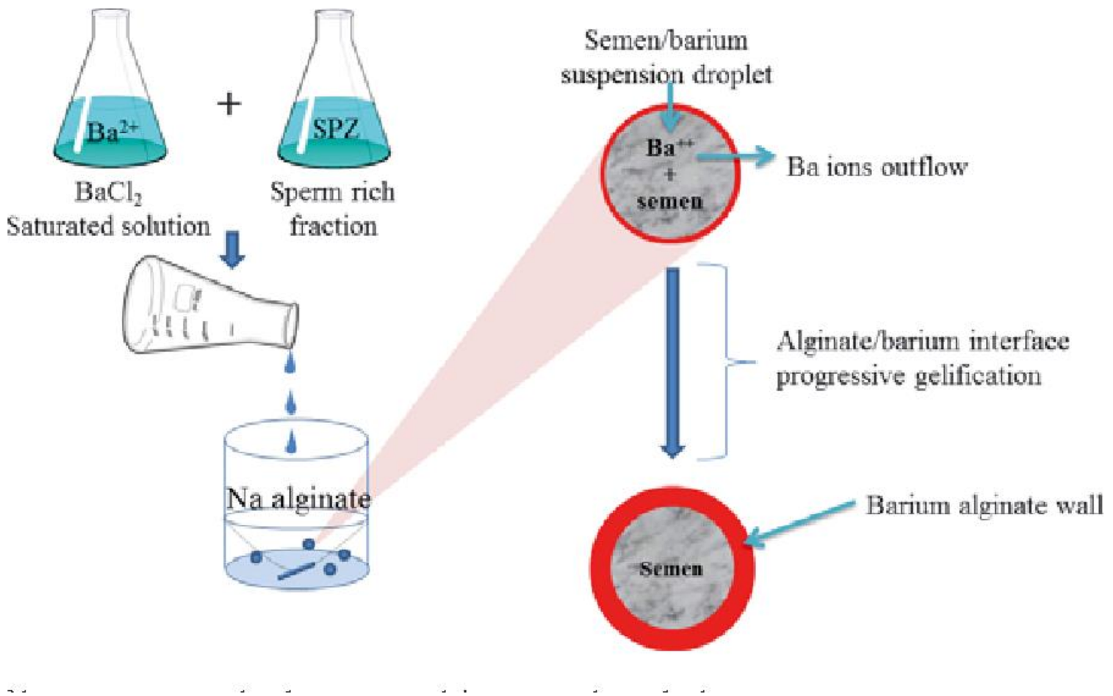

Taken from https://www.semanticscholar.org/paper/Enhancing-insemination-performance-in-pigs-through-Faustini-Vigo/496b12b10e52f4cb85f757fc0bfbba838b16bc9e

Adequacy of the applied mathematical model

- Modelling of patient specific tumours' vascularisation

(Huston research group)

- what is the purpose of the research
- Is it useful for doctors and clinitients?
- Is it bring the new value to the science?

Publishing negative experimental results

- Some journals *PLOS One* , ***Journal of Negative Results in Biomedicine***.

- in which a scientist conducts a careful experiment and finds nothing

Biological Oscillators

- The principle of phenomenological mapping

non-linearity

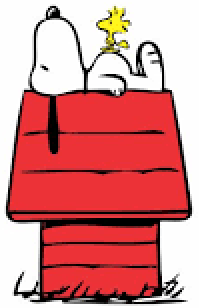

www.adesivolegal.com.br

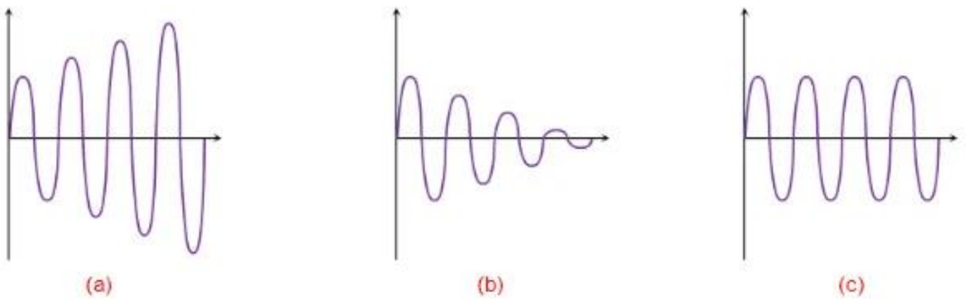

Figure 2 (a) Increasing Oscillations (b) Decaying Oscillations (c) Constant-Amplitude Oscillations

Electrical 4 U

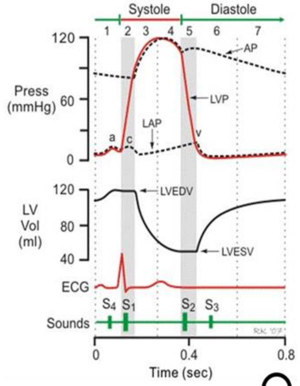

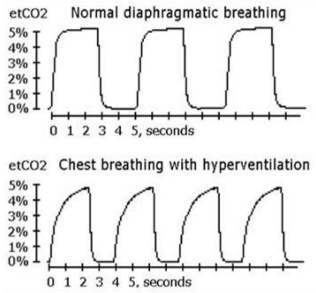

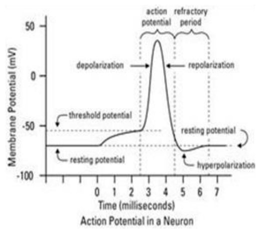

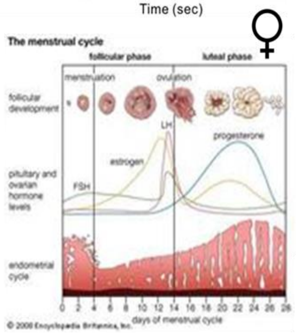

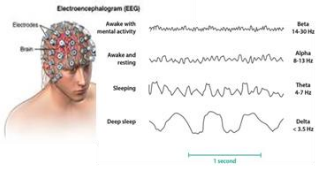

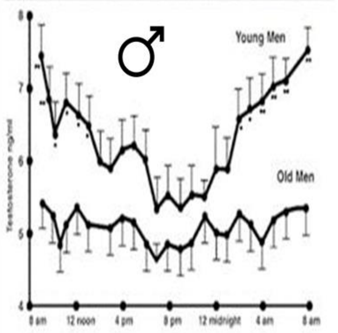

Simple harmonic oscillator

$$F = ma = m\frac{\mathrm{d}^2x}{\mathrm{d}t^2} = m\ddot{x} = -kx.$$

$$x(t) = A\cos(\omega t + \varphi),$$

$$\omega = \sqrt{\frac{k}{m}}.$$ undamped angular frequency

•k is the spring constant

Damped harmonic oscillator

$$F = -kx - c\frac{\mathrm{d}x}{\mathrm{d}t} = m\frac{\mathrm{d}^2x}{\mathrm{d}t^2},$$

$$\frac{\mathrm{d}^2x}{\mathrm{d}t^2} + 2\zeta\omega_0\frac{\mathrm{d}x}{\mathrm{d}t} + \omega_0^2 x = 0,$$

$$\zeta = \frac{c}{2\sqrt{mk}}$$ damping ratio

Driven harmonic oscillators

$$z(t) = Ae^{-\zeta\omega_0 t}\sin\left(\sqrt{1-\zeta^2}\omega_0 t + \varphi\right),$$

$$F(t) - kx - c\frac{\mathrm{d}x}{\mathrm{d}t} = m\frac{\mathrm{d}^2x}{\mathrm{d}t^2}.$$ or

$$\frac{\mathrm{d}^2x}{\mathrm{d}t^2} + 2\zeta\omega_0\frac{\mathrm{d}x}{\mathrm{d}t} + \omega_0^2 x = \frac{F(t)}{m}.$$

undamped $\longrightarrow$

$$\dot{x}\left(\ddot{x} + \alpha x + \beta x^3\right) = 0$$
$$\Rightarrow \frac{\mathrm{d}}{\mathrm{d}t}\left[\tfrac{1}{2}(\dot{x})^2 + \tfrac{1}{2}\alpha x^2 + \tfrac{1}{4}\beta x^4\right] = 0$$
$$\Rightarrow \tfrac{1}{2}(\dot{x})^2 + \tfrac{1}{2}\alpha x^2 + \tfrac{1}{4}\beta x^4 = H,$$

Duffing oscillator

$$\ddot{x} + \delta\dot{x} + \alpha x + \beta x^3 = \gamma\cos(\omega t)$$

Damped $\longrightarrow$

$$\dot{x}\left(\ddot{x} + \delta\dot{x} + \alpha x + \beta x^3\right) = 0$$
$$\Rightarrow \frac{\mathrm{d}}{\mathrm{d}t}\left[\tfrac{1}{2}(\dot{x})^2 + \tfrac{1}{2}\alpha x^2 + \tfrac{1}{4}\beta x^4\right] = -\delta(\dot{x})^2$$
$$\Rightarrow \frac{\mathrm{d}H}{\mathrm{d}t} = -\delta(\dot{x})^2 \le 0,$$

Synchronisation of biological oscillators

- Hart rate-respiration frequency

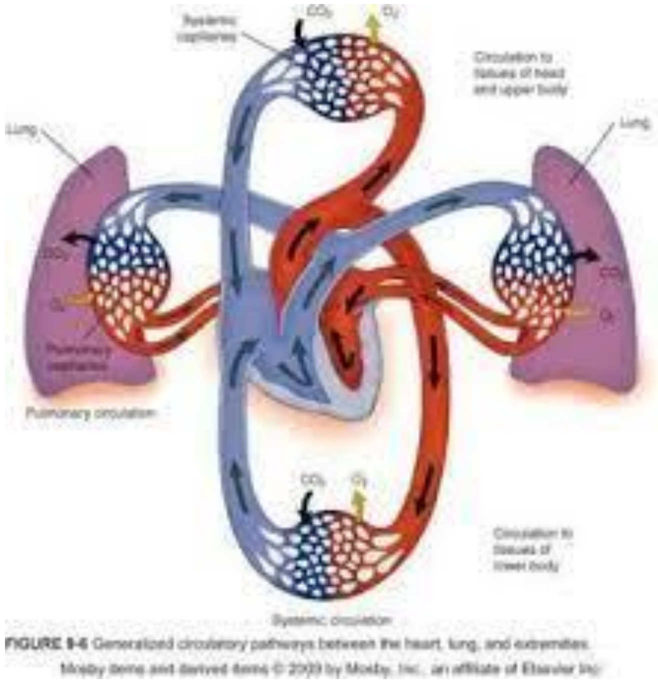

- Muscle contraction- neuronal potential

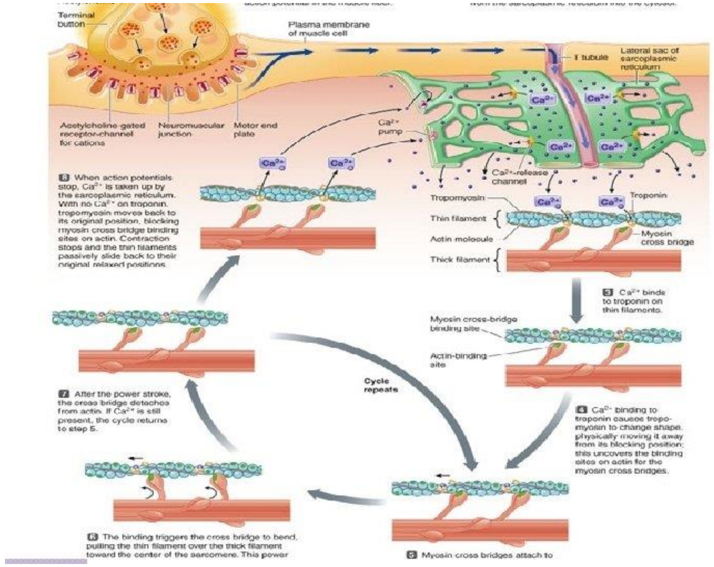

- hormones

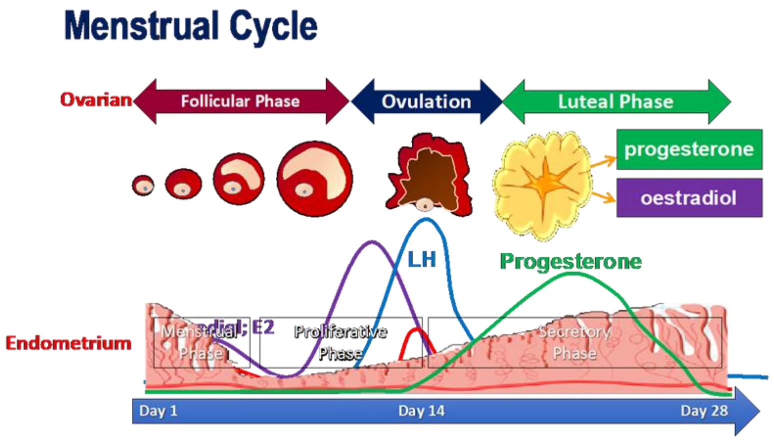

Synchronisation of biological oscillators

- Embryonal development

- Cell division

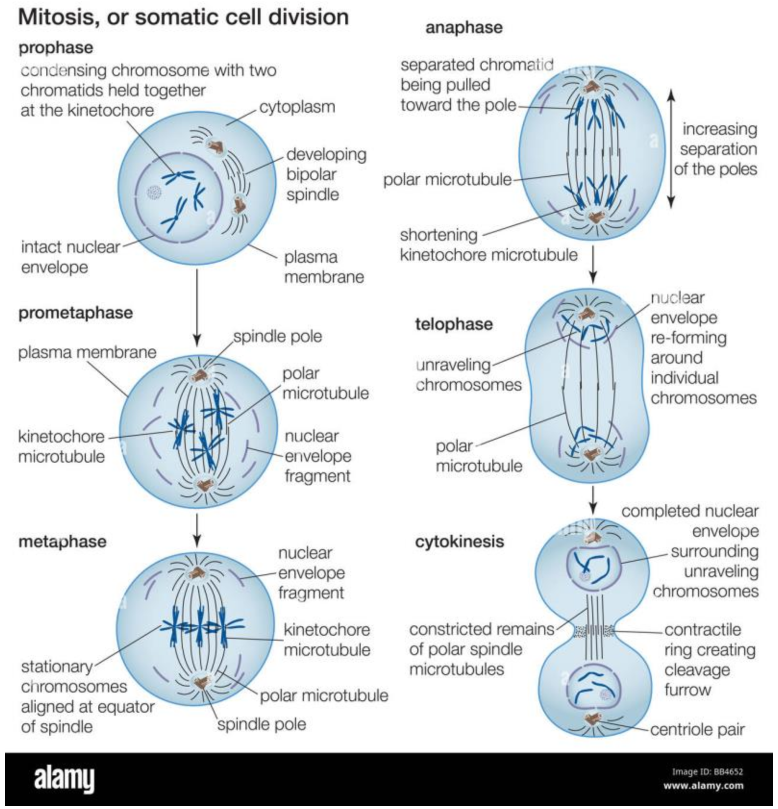

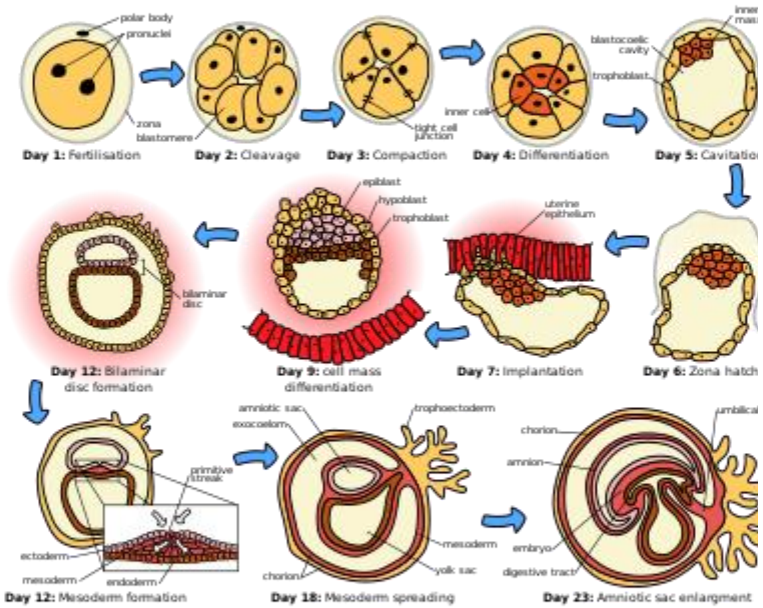

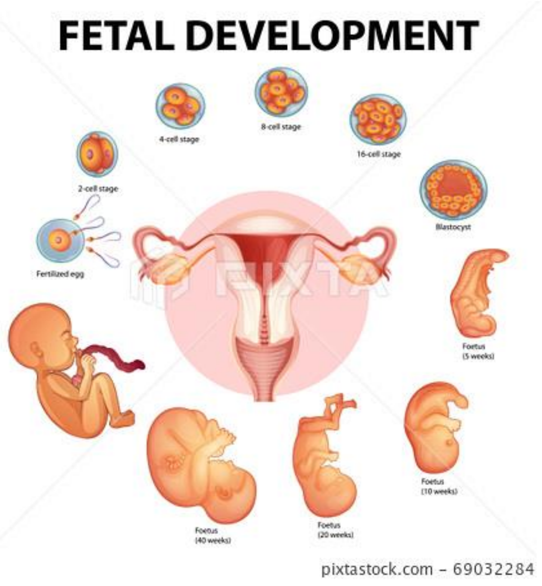

…….

Oscillators in reproductive biology

ZP as dynamical 3D structure

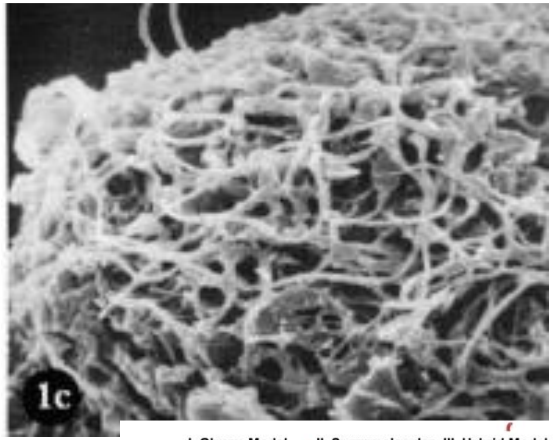

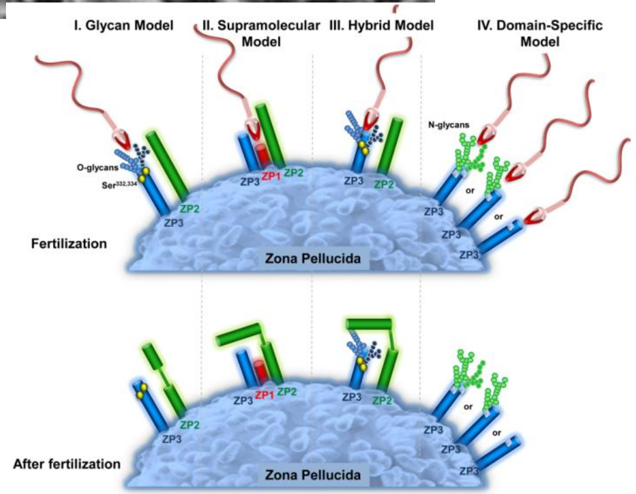

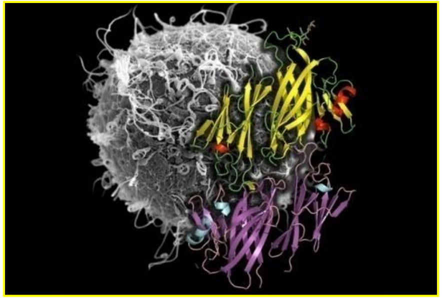

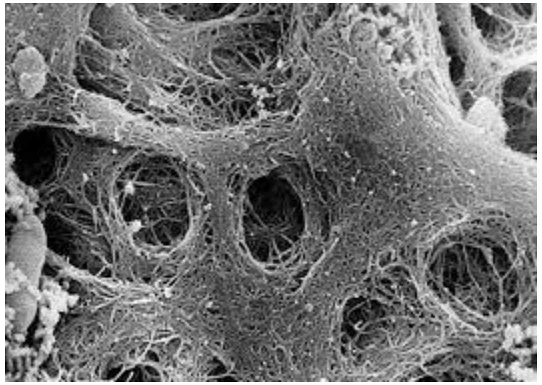

INNNR

OUTER LAYER

Labeling of mouse embryo with silicon chips

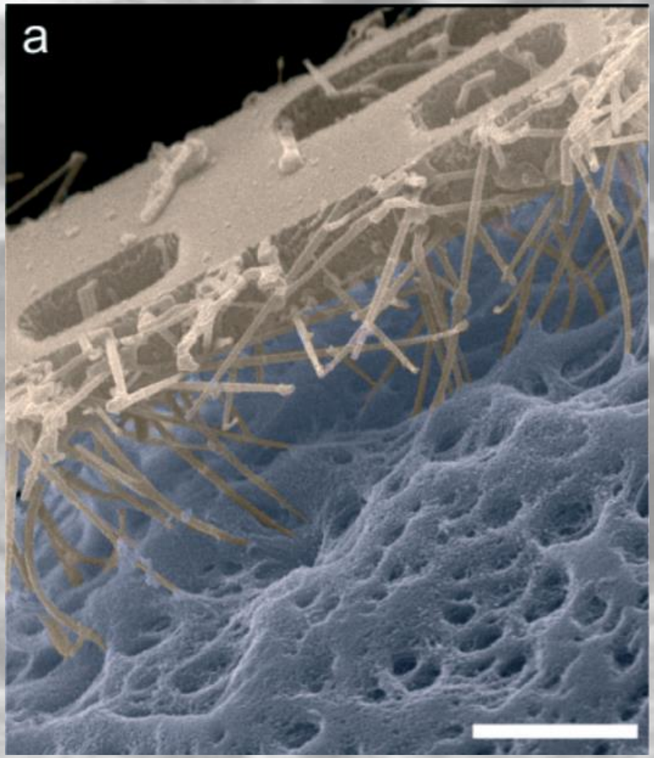

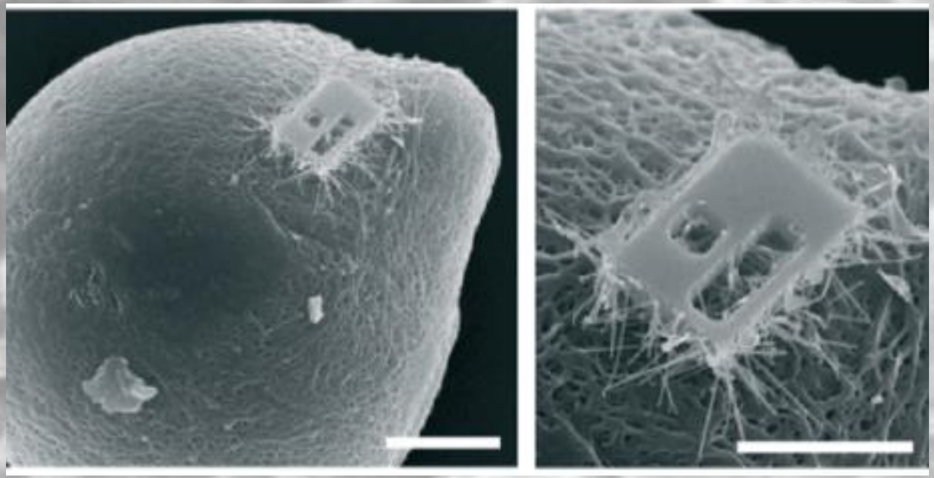

From: S. Durán, S. Novo, M. Duch, R. Gómez-Martínez, M. Fernández-Regúlez, A. San Paulo, C. Nogués, J. Esteve,a E. Ibañez and J. A. Plaza. Silicon-nanowire based attachment of silicon chips for mouse embryo labelling. . Lab Chip. 2015, 15, 1508–1514.

Mechanical properties of ZP

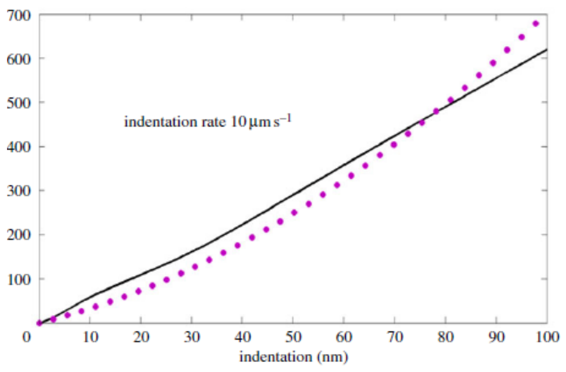

From:Boccaccio A, Lamberti L, Papi M, De Spirito M, Douet C, Goudet G, Pappalettere C. A hybrid characterization framework to determine the visco-hyperelastic properties of a porcine zona pellucida. Interface Focus 4: 20130066, 2014

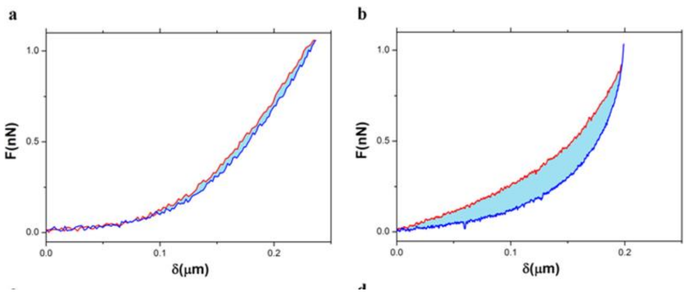

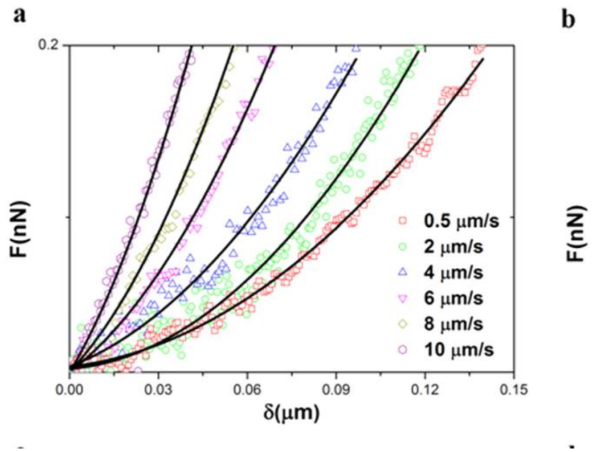

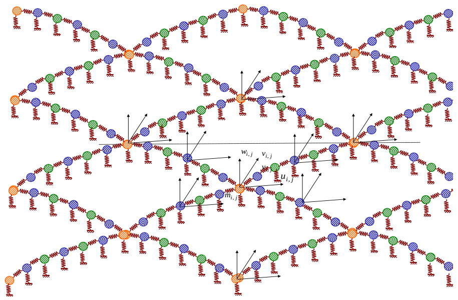

From: Papi M., Maiorana A., C, Douet C., et al., *Viscous forces are predominant in the zona pellucida mechanical resistance*. App Phy Lett Vol 102, 043703-5, 2013

Mechanical models of ZP

theoretical models of the oocyte :

- half-space model
- layered model
- shell model

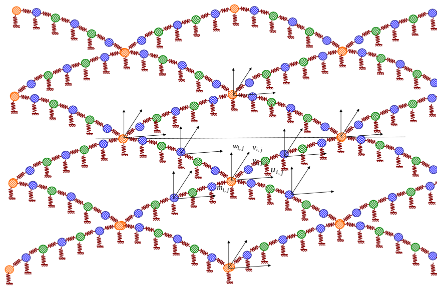

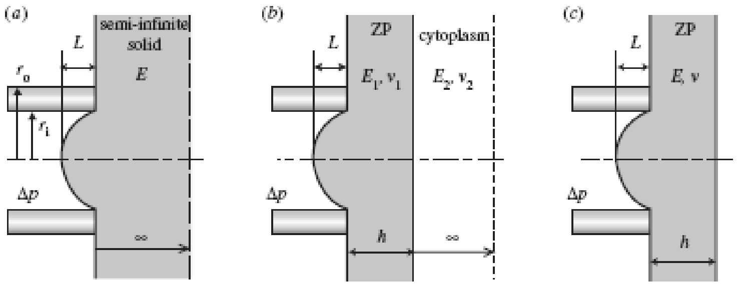

Biocapsule Elastic Models :

- the contact mechanics

Models: *Hertz's model, Sneddon model,*

- micropipette aspiration model.
- Biomembrane Point-Load Model (Sun et al, 2005).
- Discreet OSCILLATORY spherical network model of ZP

Modelling oscillatory behavior of mouse *zona-e pelucida-e* before and after fertilization

Main idea: oscillatry ineraction of oocity and sperm cells

- апроксимације модела:
- **Слободне осцилације**
- **Принудне осцилације**

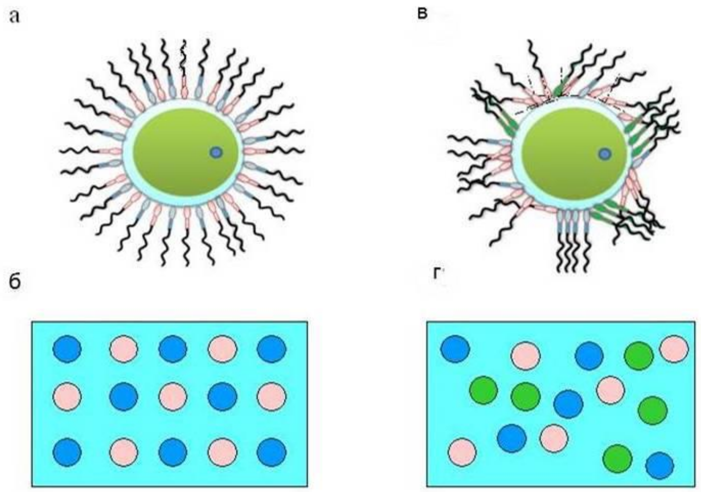

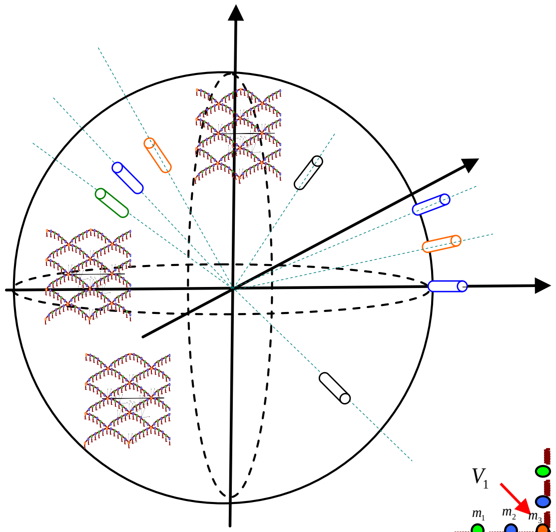

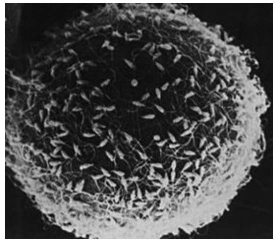

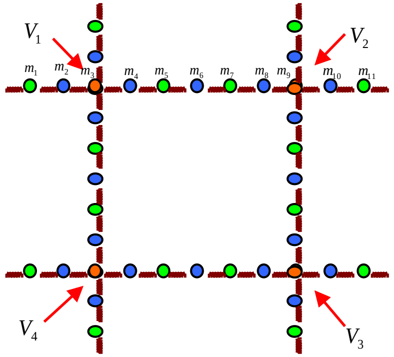

Модел осцилаторне сферне мреже *ZP* миша

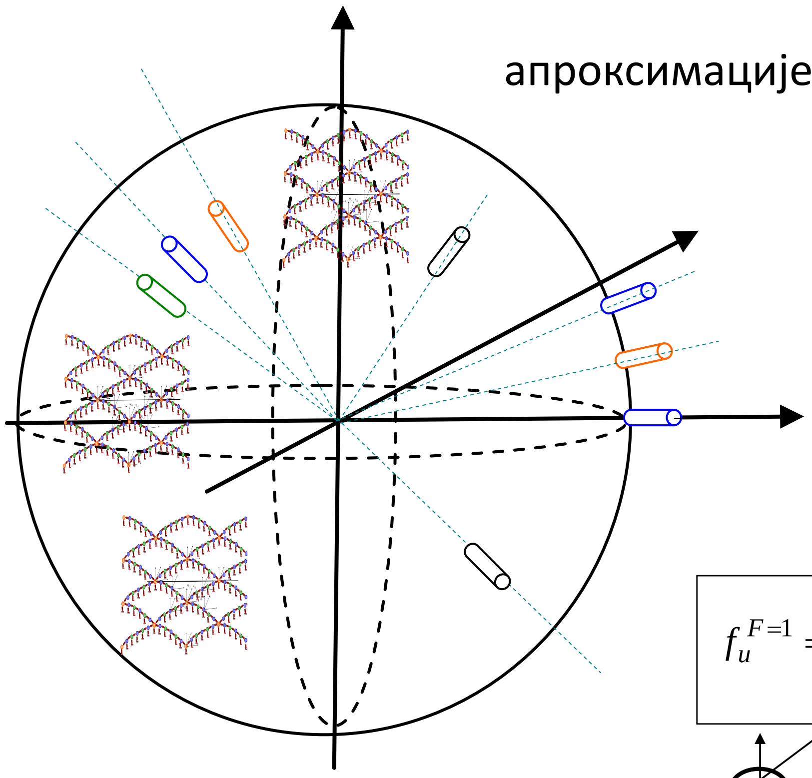

апроксимације

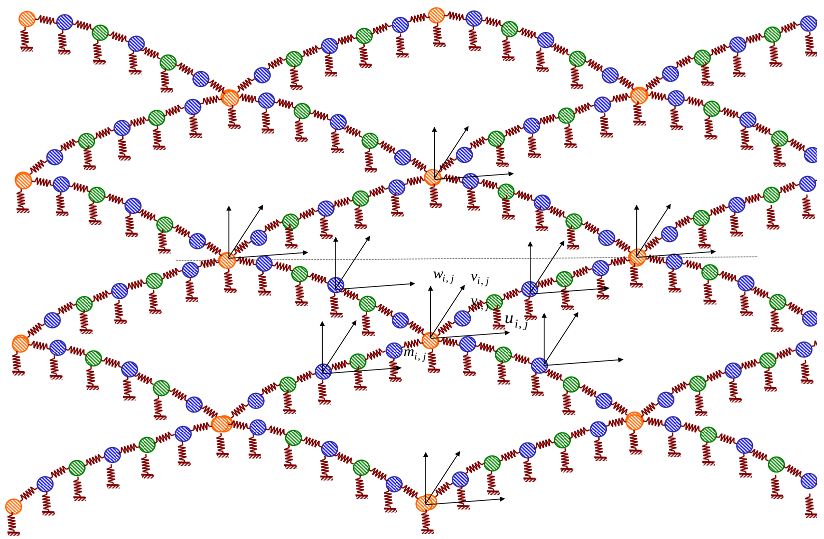

$$f_u^{F=1} = \alpha_{11} = \frac{\ell^3}{3B}$$

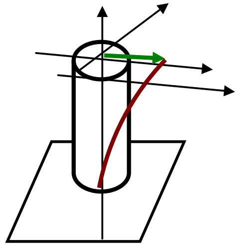

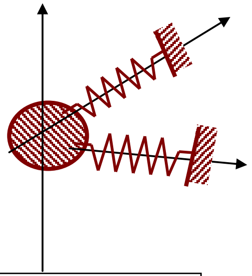

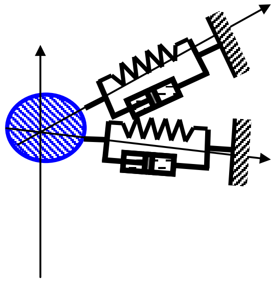

$$c_u = c_v = \frac{1}{\alpha_{11}} = \frac{3B}{\ell^3}$$

Sperm number impact

Vhp=171,1m/s

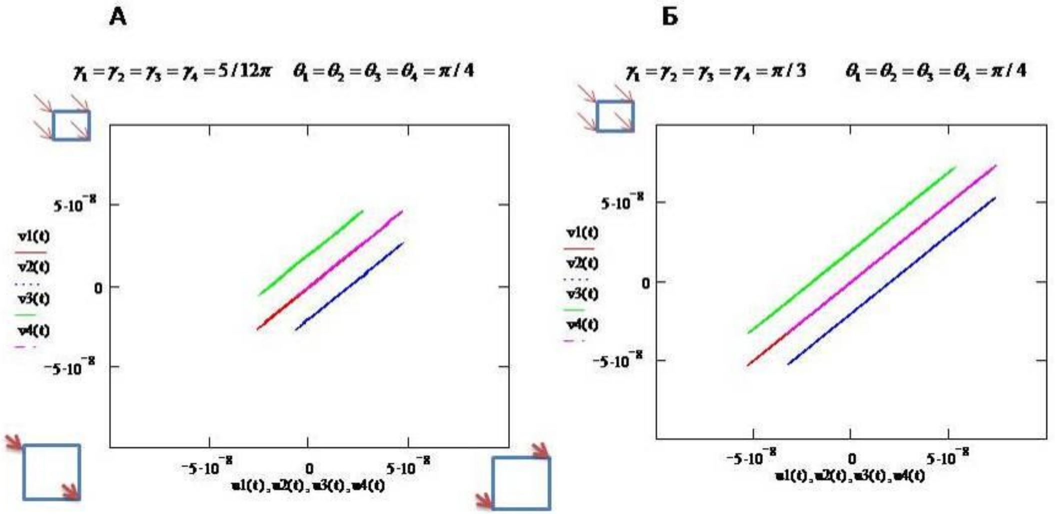

$V_{kp}=V_1=V_2=V_3=V_4=171,1\mu m/s$ $V_{kp}=V_1=V_2$ **или** $V_{kp}=V_1=V_2$

$V_{kp}=V_1=V_2=V_3=V_4=171,1\mu m/s$

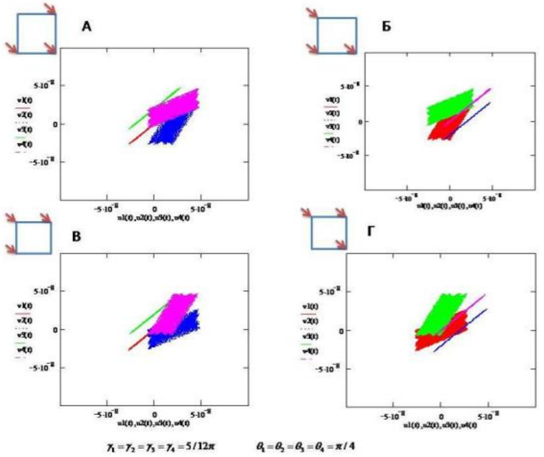

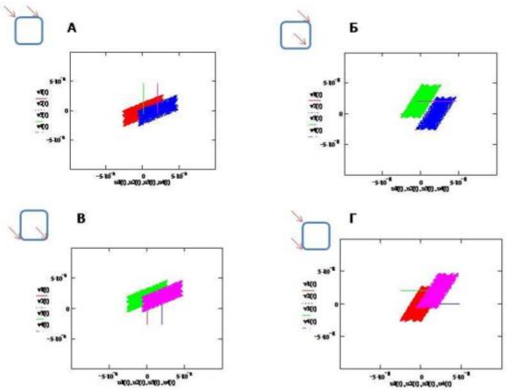

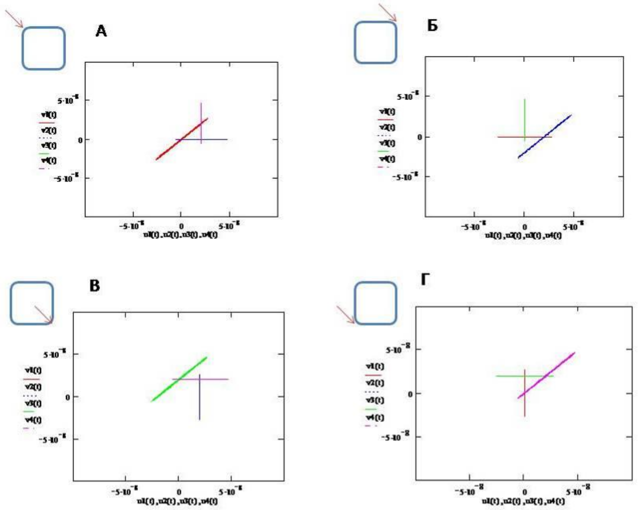

Ограничења модела:

Weak spot /area in ZP structure

Deformation work in *Zona-e Pelucida-e* during process of fertilisation

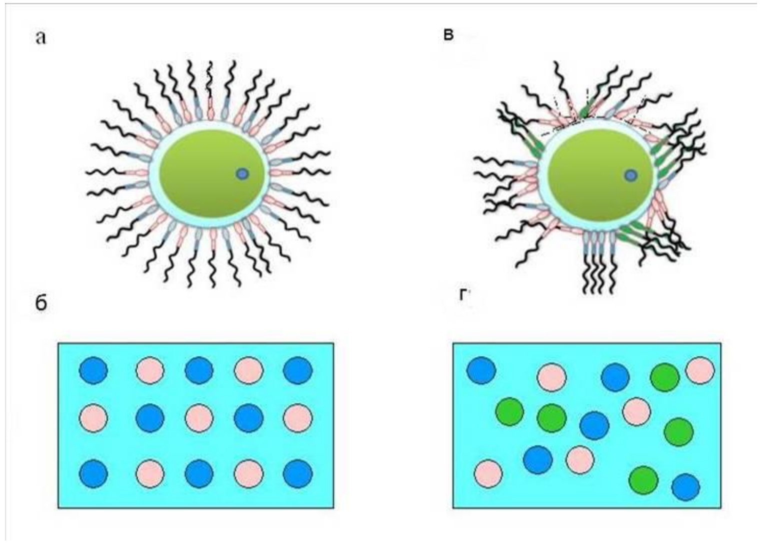

$$\sigma_r = \frac{1}{1-\psi^3}\left[\psi^3\left(1-\frac{R_o^3}{r^3}\right)p_i - \left(1-\psi^3\frac{R_o^3}{r^3}\right)p_o\right],$$

$$\sigma_c = \sigma_m = \frac{1}{1-\psi^3}\left[\psi^3\left(1+\frac{R_o^3}{r^3}\right)p_i - \left(1+\psi^3\frac{R_o^3}{r^3}\right)p_o\right],$$

$$\varepsilon_r = \frac{1}{\mathbf{G}\left(1-\psi^3\right)}\left[\frac{\psi^3 p_i - p_o}{2\left(1+3\mu k\right)} - \psi^3\frac{p_i - p_o}{2}\frac{R_o^3}{r^3}\right],$$

$$\varepsilon_c = \varepsilon_m = \frac{1}{2\mathbf{G}\left(1-\psi^3\right)}\left[\frac{\psi^3 p_i - p_o}{\left(1+3\mu k\right)} + \psi^3\frac{p_i - p_o}{2}\frac{R_o^3}{r^3}\right],$$

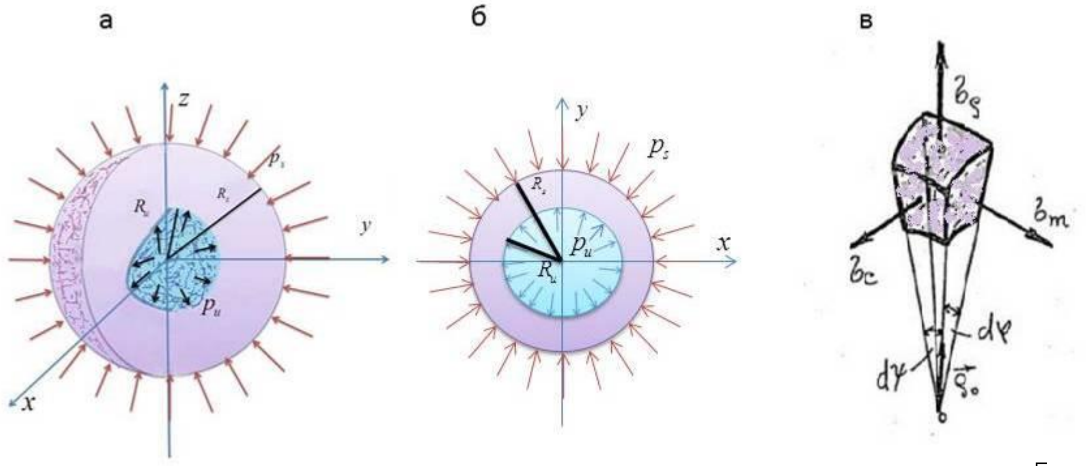

Запреминска дилатација

$$\varepsilon_V = \varepsilon_r + \varepsilon_c + \varepsilon_m = \frac{3}{2\left(1+3\mu k\right)}\frac{\psi^3 p_i - p_o}{1-\psi^3},$$

специфични деформациони рад

$$\mathbf{A}'_{def} = \frac{3}{2\mathbf{G}\left(1-\psi^3\right)^2}\left[\frac{\left(2+3\mu k\right)}{4\left(1+3\mu k\right)^2}\left(\psi^3 p_u - p_s\right)^2 + \psi^6\frac{\left(p_u - p_s\right)^2}{4}\frac{1}{r^6}\right],$$

$$\mathbf{A}_{def} = -6\mathbf{G}a^2\left[(2+3\mu k)b^2R_i^3\frac{1-\psi^3}{3} - 3c^2\frac{\psi^2-1}{R_o^2}\right], \qquad \mathbf{A}_{def} = -\frac{6}{\mathbf{G}(1-\psi^3)^2}\left[\frac{(2+3\mu k)}{12(1+3\mu k)^2}(1-\psi^3)(p_o)^2R_o^3 - \frac{3}{4}\psi^6(\psi^2-1)(p_o)^2\frac{1}{R_i^2}\right],$$

Зависност напона од растојања од центра јајне ћелије:

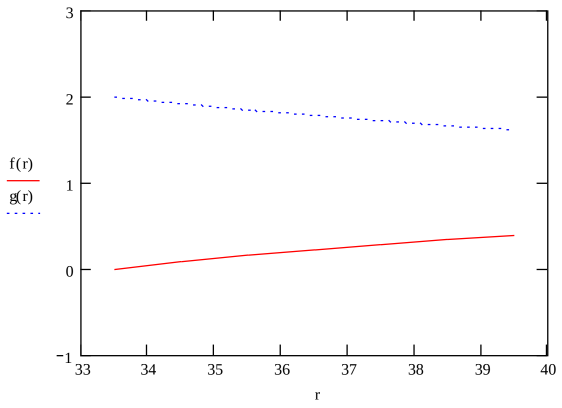

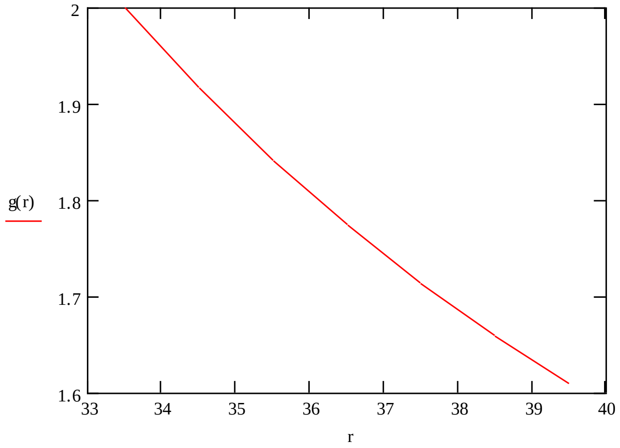

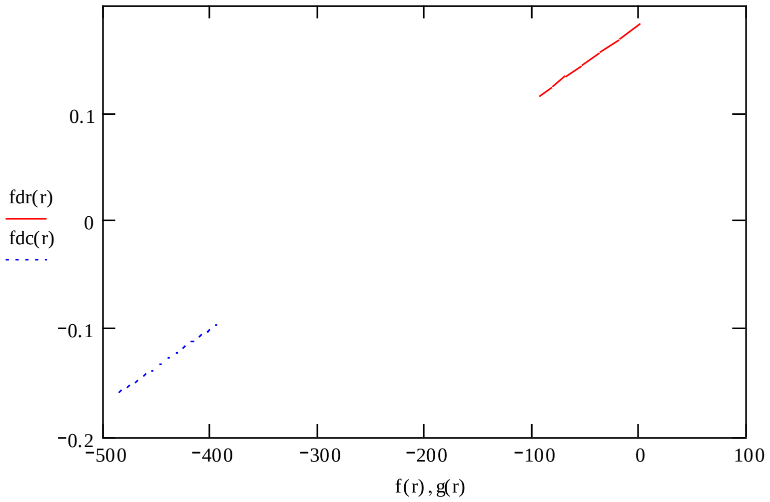

Напон/деформација

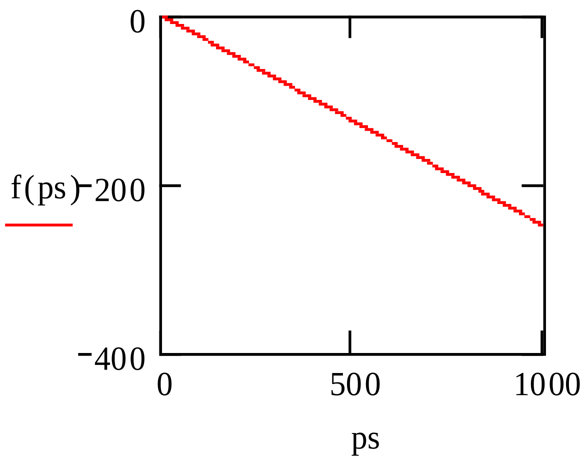

Запреминска дилатација у функцији од спољњег притиска/бр сперматозооида

The effect of friction and impact angle on the spermatozoa-oocyte local contact dynamics.

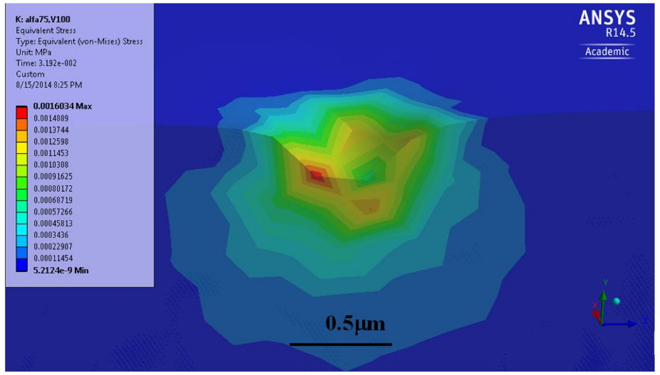

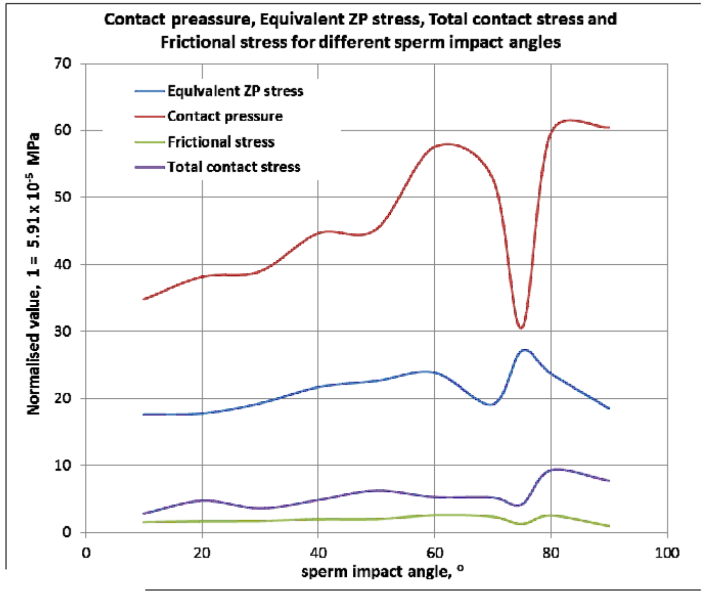

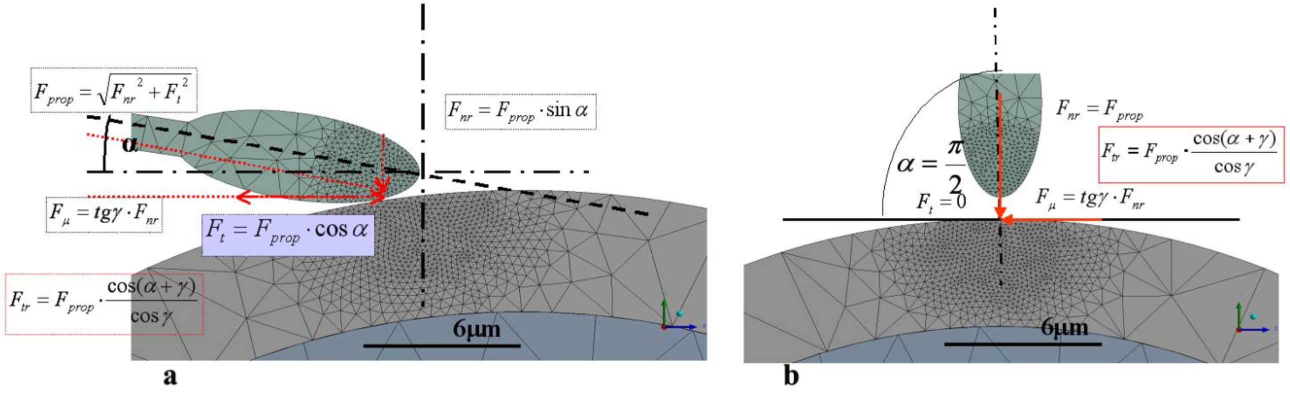

From : Hedrih, A., Banić, M.; The effect of friction and impact angle on the spermatozoa-oocyte local contact dynamics. J Theor Biol. 393: 32–42 (2016).

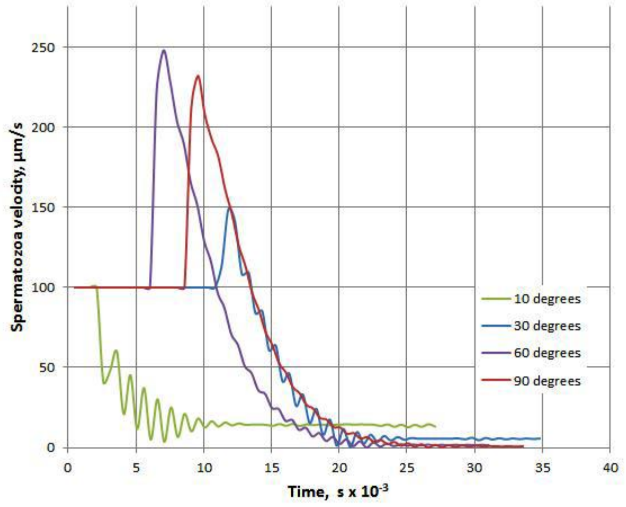

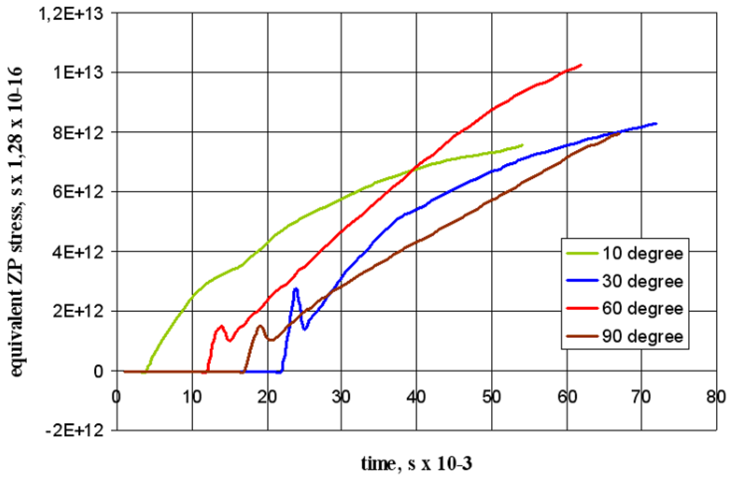

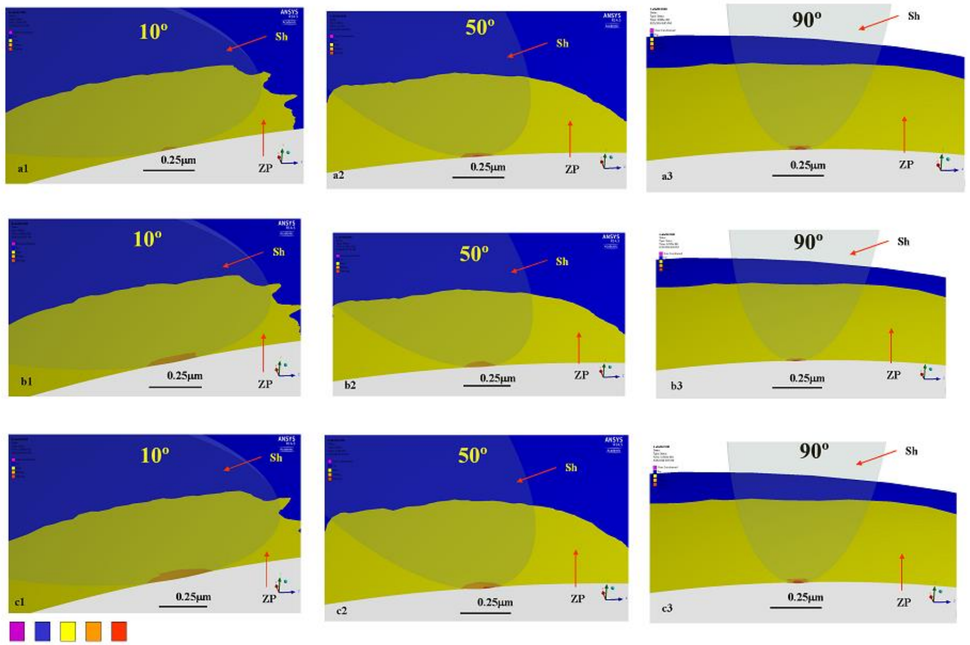

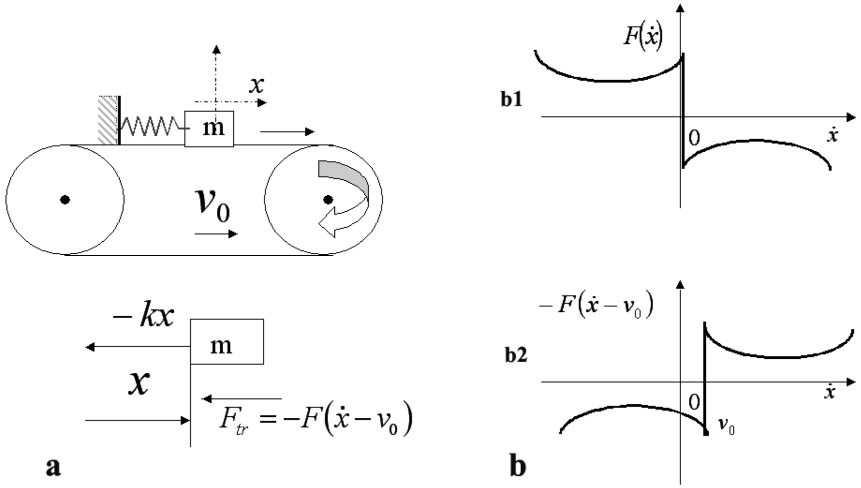

From : Hedrih, A., Banić, M.; The effect of friction and impact angle on the spermatozoa-oocyte local contact dynamics. J Theor Biol. 393: 32–42 (2016).

Осцилаторно понашање *ZP* миша након оплодње

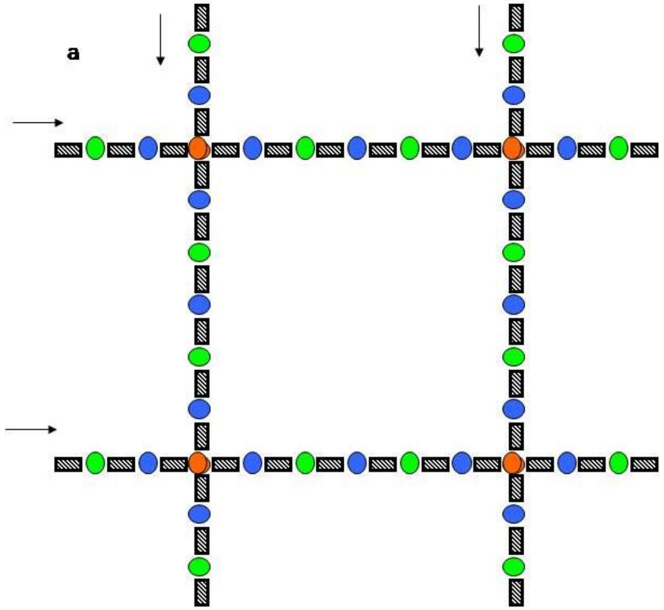

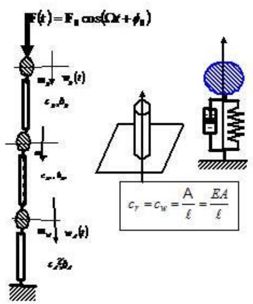

о

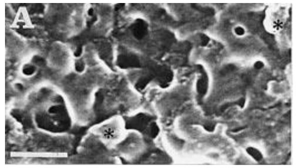

е

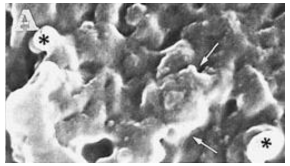

(Vanroose et, 2000)

Table 1 Young's modulus of zona pellucida

Cell stage	Number	Young's modulus (kPa) (mean ± standard deviation)
GV	30	22.8 ± 10.4 b
MII	74	8.26 ± 5.22 a
PN	66	22.3 ± 10.5 b
2 cell	41	13.8 ± 3.54 a
4 cell	19	12.6 ± 3.34 a
8 cell	6	5.97 ± 4.97 a
M	8	1.88 ± 1.34 a
EB	4	3.39 ± 1.86 a

a versus b ($P < 0.01$). EB, early blastocyst; GV, germinal vesicle; M, morulae; MII, metaphase-II; PN, pronuclear.

(Murayama et al, 2006)

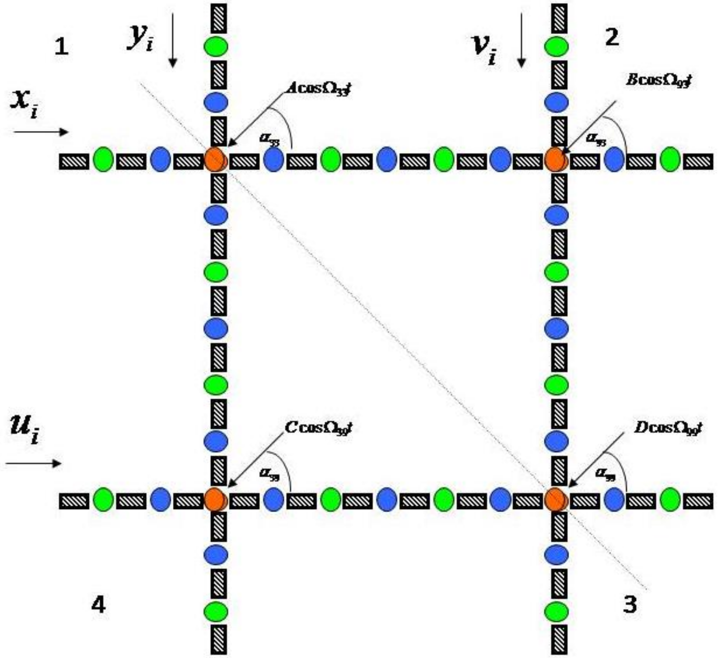

Параметри:

1. угао под којим сперматозооиди дејствују
2. фреквенција спољне принудне силе
3. амплитуда спољашње принудне силе
4. коефицијенат пригушења,
5. коефицијенат линеарне и нелинерне крутости
6. време

фреквенција спољне принудне силе

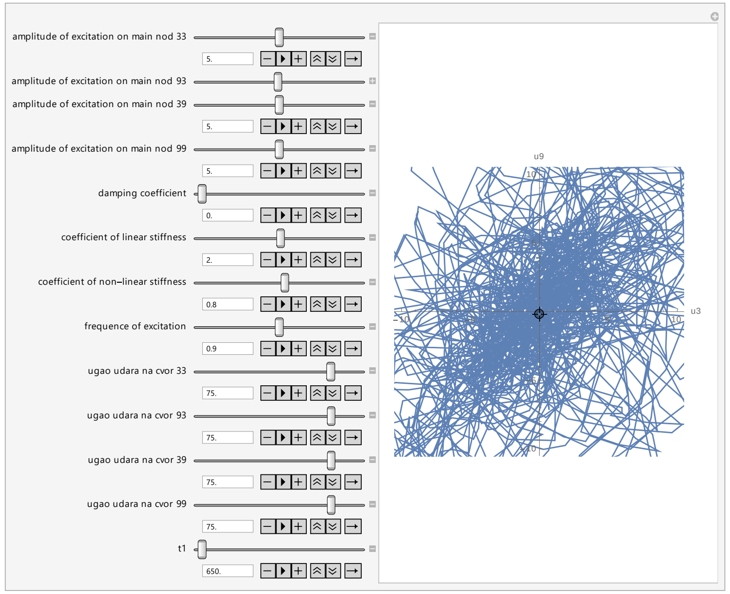

Појам *Polyspermy block*-а.

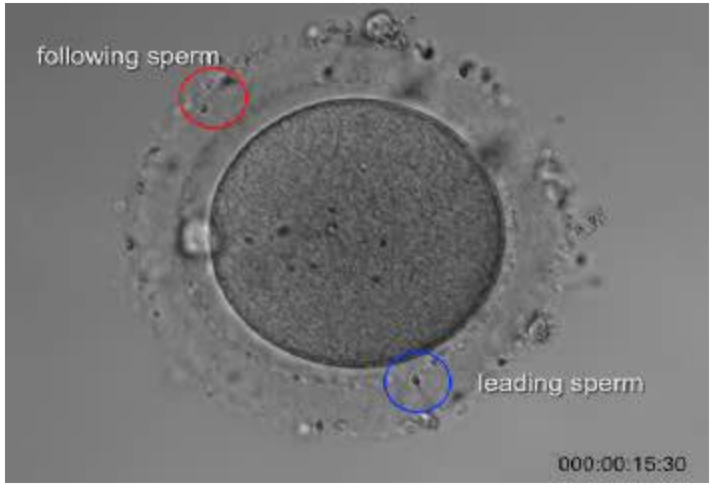

From: Yasuyuki M. et al. Possible mechanism of polyspermy block in human oocytes
observed by time-lapse cinematography. J Assist Reprod Genet (2012) 29:951–956
DOI 10.1007/s10815-012-9815-x.

коефицијент пригушења,

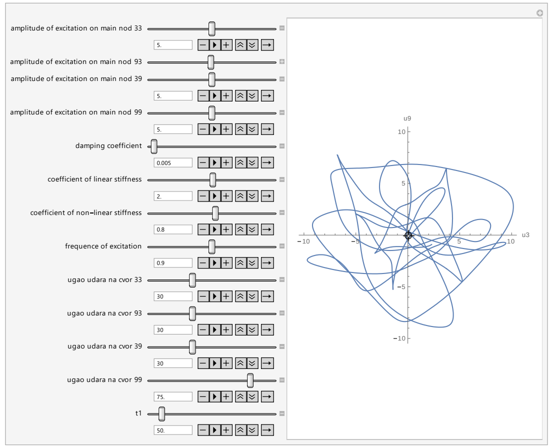

коефицијент линеарне и нелинеарне крутости

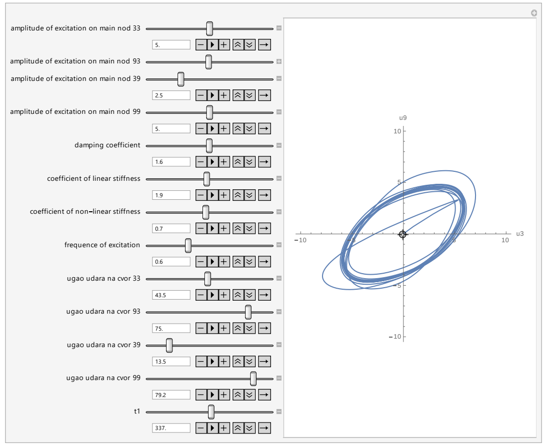

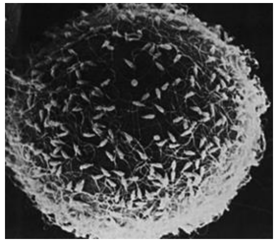

Zona pelucida as a mechano-responsive polymer

a new theory of fertilization based on coupled chemical—electrical fields

Temperature, pH and ionic strength influence biological function of ZP and its aggregate state

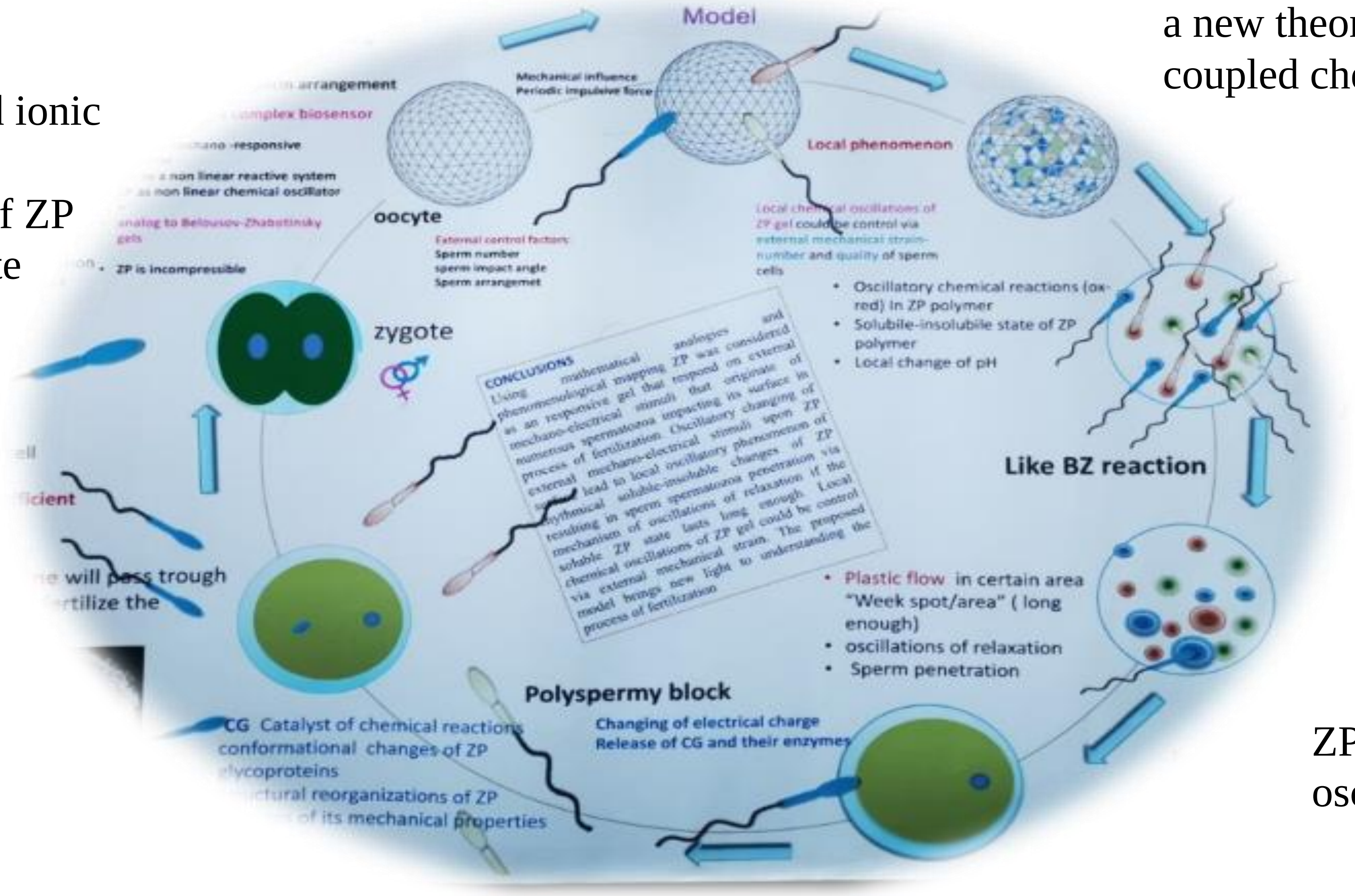

ZP as a non-linear oscillatory reactive system

Figure 8. Zona pelucida as a mechano-responsive polymer. ZP is considered as a responsive gel that responds to external mechano-electrical stimuli that originate from numerous spermatozoa impacting its surface in the process of fertilization. Oscillatory changing of external mechano-electrical stimuli upon ZP surface lead to a local oscillatory phenomenon of rhythmical soluble-insoluble changes of ZP resulting in penetration by a spermatozoid via a mechanism of oscillations of relaxation if the soluble ZP state lasts long enough. Local chemical oscillations of ZP gel could be controlled via external mechanical strain.

oscillatory model of mitotic spindle

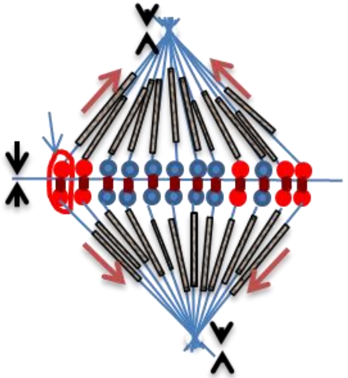

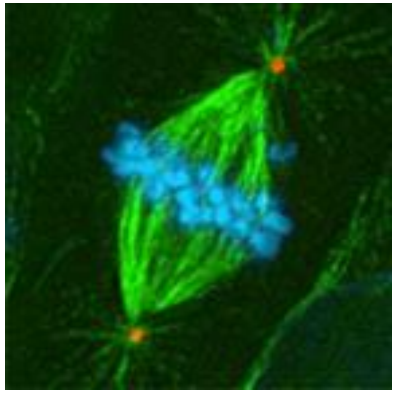

• Introduction

Cell cycle

chromosomal territories

•What is mitotic spindle?

functional genomic architecture

•age related changes in proper functioning of mitotic spindle

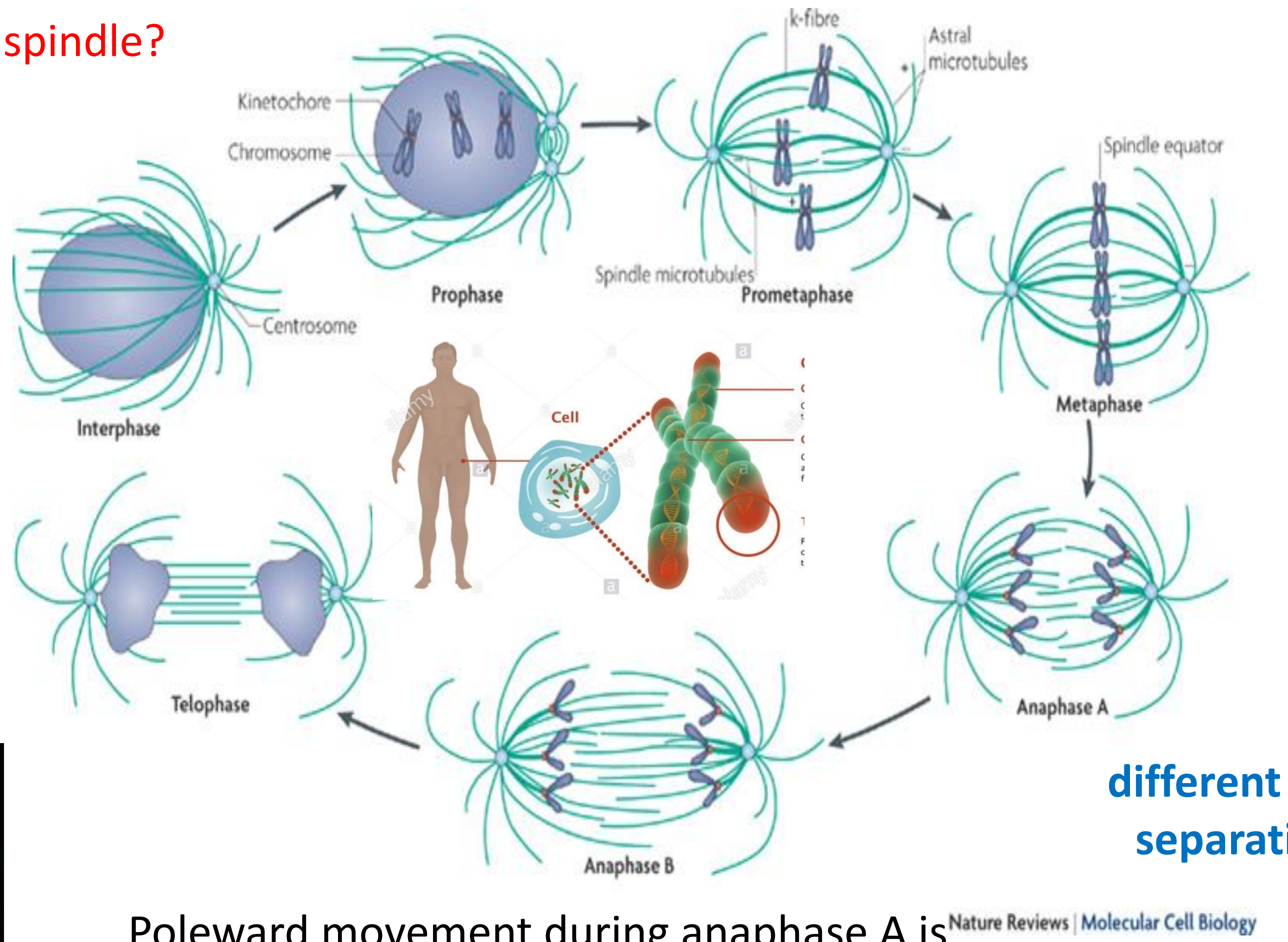

different chromatid separation times

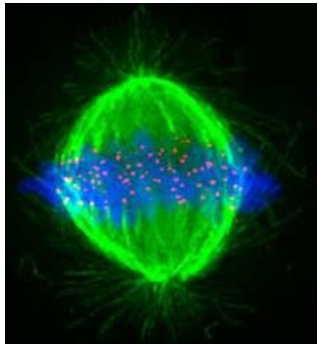

Poleward movement during anaphase A is mostly but not entirely unidirectional-it exhibits non-linear oscillatory behavior

OSCILLATORY ENERGY OF SISTER CHROMATIDS IN METAPHASE OF CELL DIVISION CYCLE

- **Influence of mass chromosome distribution**
- **Centrosome frequency**

chromosome arrangement-stochastic?

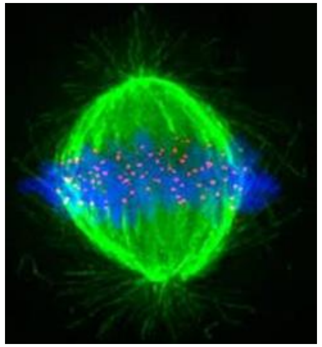

Methods

- **Basic concept of the biomechanical oscillatory model of mitotic spindle**

Assumptions:

Rheonomic centers equal, oscillate along vertical axis,
α-relatively constant,
Inclination of LEE negligable
Single frequency external excitation
In vacuum
for elastic model

$v_{O1} = \dot{y}_{gO1}$ $\qquad$ $v_{O2} = \dot{y}_{gO2}$

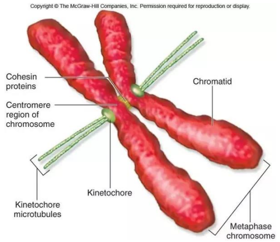

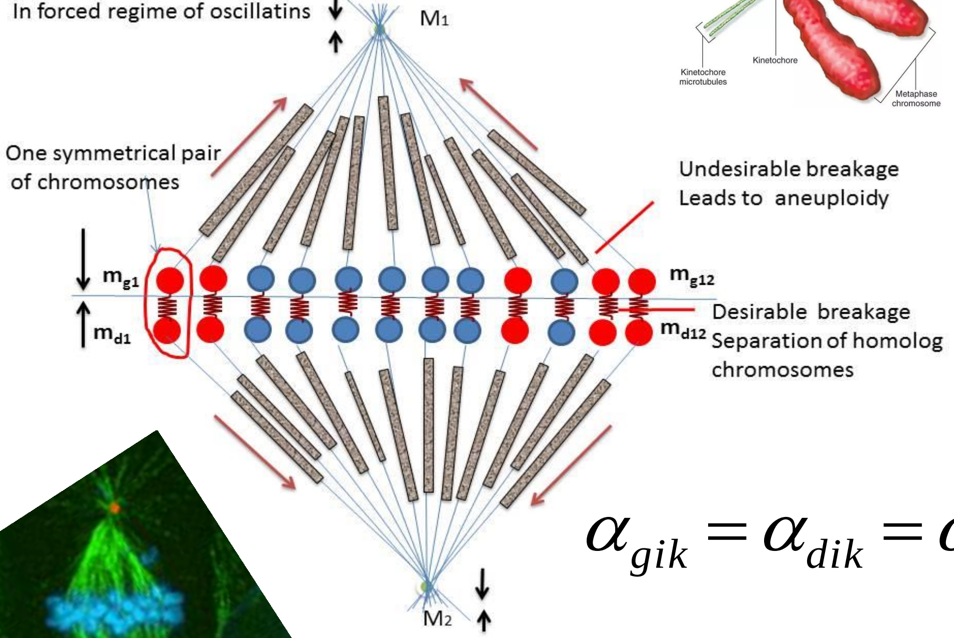

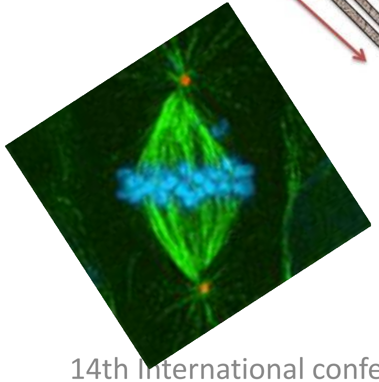

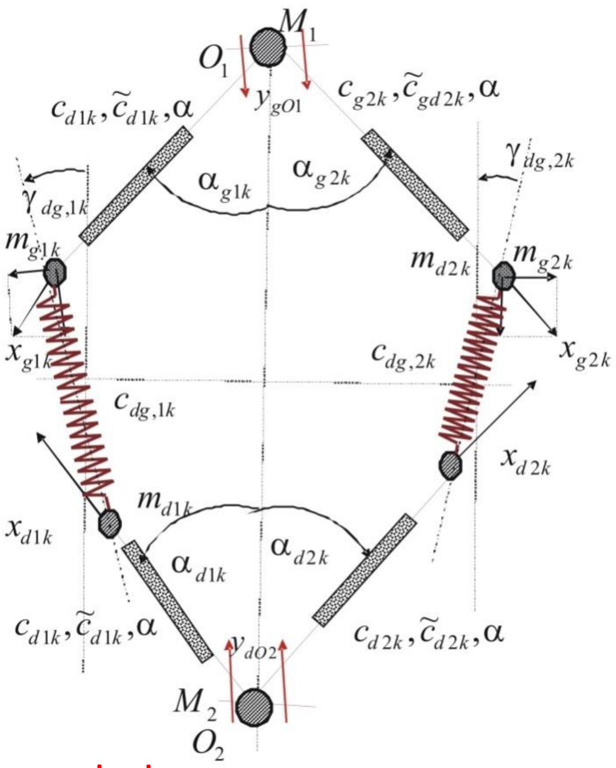

$$\alpha_{gik} = \alpha_{dik} = \alpha_{ik}$$

mitotic spindle as a system of coupled oscillators

relative and transfer velocity

Oscillatory motions of chromosomes

Square of absolute velocity of one homologue chromosome/ -th material particle in each subset

$$v_{gik}^2 = \left(\dot{x}_{gik} + \dot{y}_{gO1}\cos\alpha_{gik}\right)^2 + \left(\dot{y}_{gO1}\sin\alpha_{gik}\right)^2$$

$$v_{dik}^2 = \left(\dot{x}_{dik} + \dot{y}_{dO2}\cos\alpha_{dik}\right)^2 + \left(\dot{y}_{dO2}\sin\alpha_{dik}\right)^2$$

Approximate value of elongation of standard light linear elastic element that interconnect pairs of homologues chromosomes

$$\Delta\ell_{ik} \approx -\left[\left(y_{gO1} + y_{dO1}\right) + \left(x_{gik}\sin\alpha_{gik} + x_{dik}\sin\alpha_{dik}\right)\right]$$

Mechanical energies for each pair of homologue chromosomes in biomechanical model of mitotic spindle

$$\mathbf{E}_{K,ik}=\frac{1}{2}m_{uik}\left[\left(\dot{x}_{uik}+\dot{y}_{uO1}\cos\alpha_{uik}\right)^2+\left(\dot{y}_{uO1}\sin\alpha_{uik}\right)^2\right]+\frac{1}{2}M_u\left(\dot{y}_{uO1}\right)^2+$$

$$+\frac{1}{2}m_{dik}\left[\left(\dot{x}_{dik}+\dot{y}_{dO2}\cos\alpha_{dik}\right)^2+\left(\dot{y}_{dO2}\sin\alpha_{dik}\right)^2\right]+\frac{1}{2}M_d\left(\dot{y}_{dO2}\right)^2$$

$$E_p=\frac{1}{2}c_{uik}x^2{}_{uik}+\frac{1}{2}c_{dik}x^2{}_{dik}+\frac{1}{2}c_{ik}[(y_{uO1}+y_{dO1})+(x_{uik}\sin\alpha_{uik}+x_{dik}\sin\alpha_{dik})]^2$$

$$i=1,2...20$$

$$E_{T,ik}=E_{k,ik}+E_{p,ip}$$

Pairs of coupled fractional order differential equations could be solved independently from other coupled pairs of the mitotic spindle oscillatory system

$$\ddot{x}_{gik}+\left(\omega_{gik}^{2}+\widehat{\omega}_{gik}^{2}\sin^{2}\alpha_{gik}\right)x_{gik}+\left(\widehat{\omega}_{gik}^{2}\sin\alpha_{dik}\sin\alpha_{gik}\right)x_{dik}+\widetilde{\omega}_{gik}^{2}\left(\mathsf{D}_{t}^{\alpha}\left[x_{gik}\right]\right)=$$
$$=\left(\Omega_{g}^{2}h_{0,gik}-\widehat{\omega}_{gik}^{2}\widetilde{h}_{0,gik}\right)\cos\Omega_{g}t-\widehat{\omega}_{gik}^{2}\widetilde{\widetilde{h}}_{0,gik}\cos\Omega_{d}t$$

$$\ddot{x}_{dik}+\left(\omega_{dik}^{2}+\widehat{\omega}_{dik}^{2}\sin^{2}\alpha_{dik}\right)x_{dik}+\widetilde{\omega}_{dik}^{2}\left(\mathsf{D}_{t}^{\alpha}\left[x_{gik}\right]\right)-\left(\widehat{\omega}_{dik}^{2}\sin\alpha_{gik}\sin\alpha_{dik}\right)x_{gik}=$$
$$=\left(\Omega_{d}^{2}h_{0,dik}+\widehat{\omega}_{dik}^{2}\widetilde{h}_{0,dik}\right)\cos\Omega_{d}t+\widehat{\omega}_{dik}^{2}\widetilde{\widetilde{h}}_{0,dik}\cos\Omega_{g}t$$

$$Q_{gO1}=\frac{d}{dt}\left(\frac{\partial\mathbf{E}_{K}}{\partial\dot{y}_{gO1}}\right)-\frac{\partial\mathbf{E}_{K}}{\partial y_{gO1}}+\frac{\partial\left(\mathbf{E}_{P}+\mathbf{E}_{PE}\right)}{\partial y_{gO1}}+\frac{\partial\mathbf{P}_{W}}{\partial\left(\mathsf{D}_{t}^{\alpha}\left[y_{gO1}\right]\right)}$$

$$Q_{d2}=\frac{d}{dt}\left(\frac{\partial\mathbf{E}_{K}}{\partial\dot{y}_{dO2}}\right)-\frac{\partial\mathbf{E}_{K}}{\partial y_{dO2}}+\frac{\partial\left(\mathbf{E}_{P}+\mathbf{E}_{PE}\right)}{\partial y_{dO2}}+\frac{\partial\mathbf{P}_{W}}{\partial\left(\mathsf{D}_{t}^{\alpha}\left[y_{dO1}\right]\right)}$$

$$\omega_{gik}^{2}=\frac{c_{gik}}{m_{gik}}\qquad\widetilde{\omega}_{gik}^{2}=\frac{\widetilde{c}_{gik}}{m_{gik}}\qquad h_{0,gik}=y_{go}\cos\alpha_{gik}$$

$$\omega_{dik}^{2}=\frac{c_{dik}}{m_{dik}}\qquad\widetilde{\omega}_{dik}^{2}=\frac{\widetilde{c}_{dik}}{m_{dik}}\qquad h_{0,dik}=y_{do}\cos\alpha_{dik}$$

$$\widehat{\omega}_{gik}^{2}=\frac{c_{ik}}{m_{gik}}\qquad\widehat{\omega}_{dik}^{2}=\frac{c_{ik}}{m_{dik}}\qquad\widetilde{h}_{0,dik}=y_{d0}\sin\alpha_{dik}$$

$$\widetilde{h}_{0,gik}=y_{g0}\sin\alpha_{gik}\qquad\widetilde{\widetilde{h}}_{0,gik}=y_{d0}\sin\alpha_{gik}\qquad\widetilde{\widetilde{h}}_{0,dik}=y_{g0}\sin\alpha_{dik}$$

Particular solutions of modified ordinary differential equations

$$x_{Pgik} = D_{gik}\cos\Omega_g t + \tilde{D}_{gik}\cos\Omega_d t$$

$$x_{Pdik} = D_{dik}\cos\Omega_g t + \tilde{D}_{dik}\cos\Omega_d t$$

$$\left[\left(\omega_{gik}^2 + \hat{\omega}_{gik}^2 \sin^2\alpha_{gik}\right) - \Omega_g^2\right] D_{gik} + \left(\hat{\omega}_{gik}^2 \sin\alpha_{dik}\sin\alpha_{gik}\right) D_{dik} = \left(\Omega_g^2 h_{0,gik} - \hat{\omega}_{gik}^2 \tilde{h}_{0,gik}\right)$$

$$\left[\left(\omega_{gik}^2 + \hat{\omega}_{gik}^2 \sin^2\alpha_{gik}\right) - \Omega_d^2\right] \tilde{D}_{gik} + \left(\hat{\omega}_{gik}^2 \sin\alpha_{dik}\sin\alpha_{gik}\right) \tilde{D}_{dik} = -\hat{\omega}_{gik}^2 \tilde{\tilde{h}}_{0,gik}$$

$$\left[\left(\omega_{dik}^2 + \hat{\omega}_{dik}^2 \sin^2\alpha_{dik}\right) - \Omega_g^2\right] D_{dik} + \left(\hat{\omega}_{dik}^2 \sin\alpha_{gik}\sin\alpha_{dik}\right) D_{gik} = \hat{\omega}_{dik}^2 \tilde{h}_{0,dik}$$

$$\left[\left(\omega_{dik}^2 + \hat{\omega}_{dik}^2 \sin^2\alpha_{dik}\right) - \Omega_d^2\right] \tilde{D}_{dik} + \left(\hat{\omega}_{dik}^2 \sin\alpha_{gik}\sin\alpha_{dik}\right) \tilde{D}_{gik} = \left(\Omega_d^2 h_{0,dik} + \hat{\omega}_{dik}^2 \tilde{\tilde{h}}_{0,dik}\right)$$

Numerical analysis

Data:

Chromosomal mass for mouse chromosome were taken from ref (Ortega et al, 1957).

From $4.5/2*10^{-15}$kg to $1.6/2*10^{-15}$kg

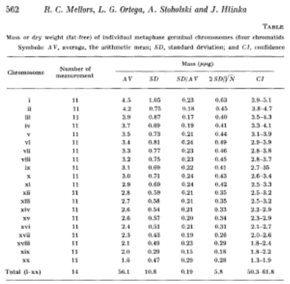
562 R. C. Mellors, L. G. Ortega, A. Stoholski and J. Hlinka

TABLE

Mass or dry weight (fat-free) of individual metaphase germinal chromosomes (four chromatids

Symbols: AV, average, the arithmetic mean; SD, standard deviation; and CI, confidence

Chromosome	Number of measurement	Mass (μμg)				
		AV	SD	SD/AV	$2SD/\sqrt{N}$	CI
i	11	4.5	1.05	0.23	0.63	3.9–5.1
ii	11	4.2	0.75	0.18	0.45	3.8–4.7
iii	11	3.9	0.67	0.17	0.40	3.5–4.3
iv	11	3.7	0.69	0.19	0.41	3.3–4.1
v	11	3.5	0.73	0.21	0.44	3.1–3.9
vi	11	3.4	0.81	0.24	0.49	2.9–3.9
vii	11	3.3	0.77	0.23	0.46	2.8–3.8
viii	11	3.2	0.75	0.23	0.45	2.8–3.7
ix	11	3.1	0.69	0.22	0.41	2.7–35
x	11	3.0	0.71	0.24	0.43	2.6–3.4
xi	11	2.9	0.69	0.24	0.42	2.5–3.3
xii	11	2.8	0.59	0.21	0.35	2.5–3.2
xiii	11	2.7	0.58	0.21	0.35	2.5–3.2
xiv	11	2.6	0.54	0.21	0.33	2.3–2.9
xv	11	2.6	0.57	0.20	0.34	2.3–2.9
xvi	11	2.4	0.51	0.21	0.31	2.1–2.7
xvii	11	2.3	0.43	0.19	0.26	2.0–2.6
xviii	11	2.1	0.49	0.23	0.29	1.8–2.4
xix	11	2.0	0.29	0.15	0.18	1.8–2.2
xx	11	1.6	0.47	0.29	0.28	1.3–1.9
Total (i–xx)	14	56.1	10.8	0.19	5.8	50.3–61.8

Rigidity of eukaryote metaphase chromosomes: $Cc = 1.413 * 10^{-3}$N/m

Calculated from formula:

$Cc = Ecr^2\pi/lc$

Young modulus of metaphase chromosomes elasticity:

$Ec=10^3$Pa

$r=3\mu m$

$lc=20\mu m$

taken from (Houchmandzadeh et al, 1997)

Rigidity for microtubules at 37° C:

Calculated from: $cm = Em(R_o^2 - R_i^2)\pi/lm$

Young modulus of microtubules at 37° C: $Cm = 3.44 * 10^{-6}$N/m

$Em=1,9*10^8$Pa

$R_{i=18nm}$

$R_{o=30nm}$

$_{lm=100\mu m}$data taken from ref (Kis et al, 2008)

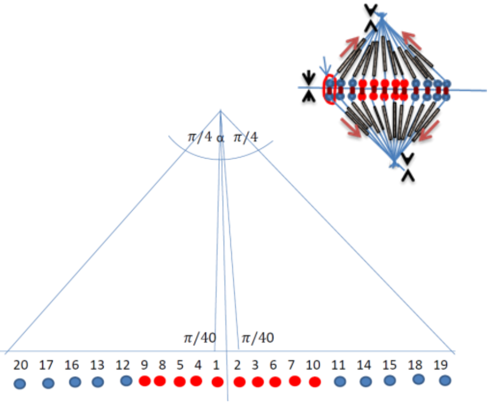

- Chromosomal mass
- Rigidity of eukaryote metaphase chromosomes
- Rigidity for microtubules at 37° C
- Centrosome mass
- Centrosome amplitude oscillations
- Centrosome - Rheonomic centers circular frequency
- Ange of mitotic spindle

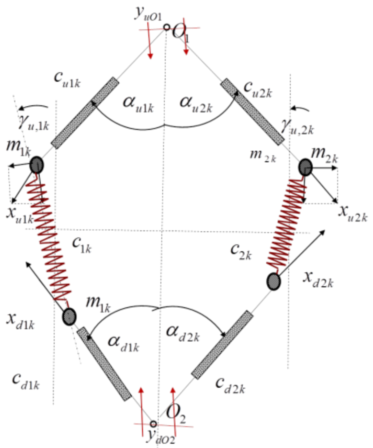

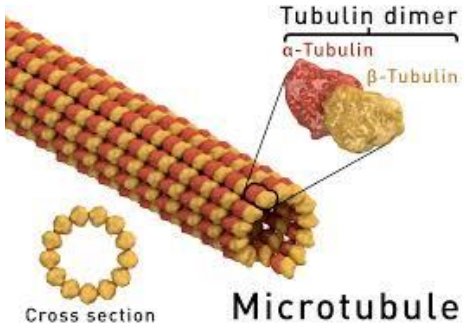

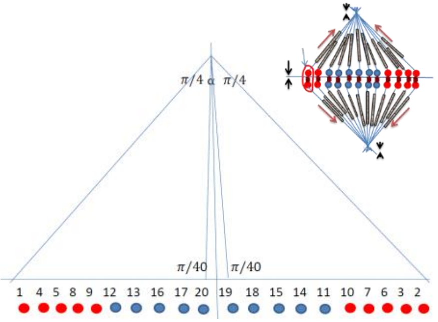

Numerical analysis

Data:

Rheonomic centers circular frequency

was calculated according to the data for from (Maly, 2013) (2π/T, T1=20s, T2=15s).

$\Omega_1 = 0.419$ 1/s $\Omega_1 = 0.314$ 1/s

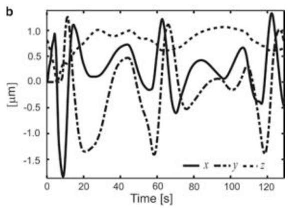

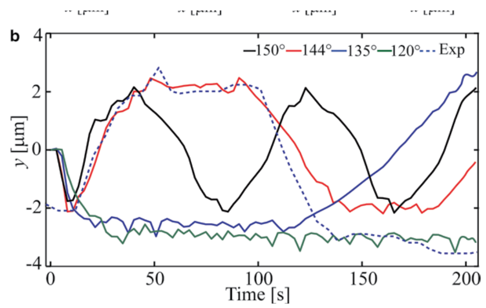

Centrosome mass

was calculated from centrosome volume

1,5μm^3 from http://www.proteinatlas.org/humancell/

and centrosome density - (density was taken approximatively as data for density for cell organelle-mitochondria 1,05g/ml)

1.575*10^{-15}kg (Milo and Phillips, 2016).

Centrosome amplitude oscillations

was taken from (Kuhn and Poenie, 2002)

(2.1μm=2.1/2*10^{-6}kg)

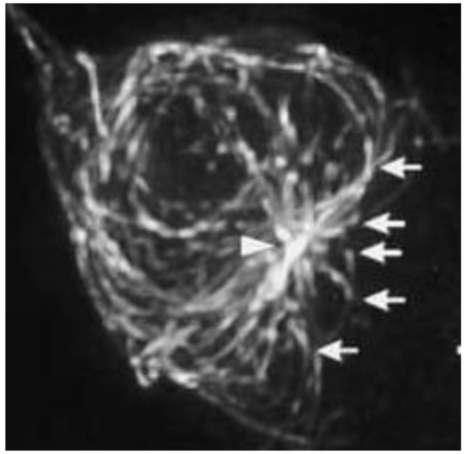

Ange of mitotic spindle

Take as π/2, equal distribution angles

Results

Total mechanical energy of 10 pairs of homologue chromosomes in the system of mitotic spindle

Case

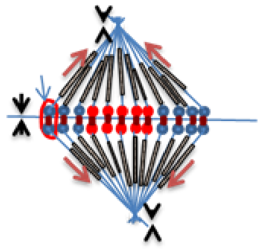

Same frequency of rheonomic centers $\Omega_1 = 0.419$ 1/s

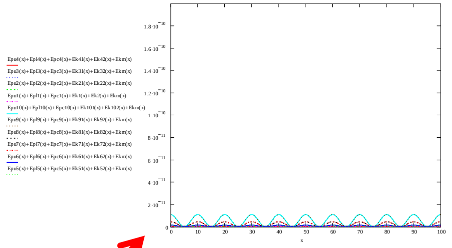

central

peripheral

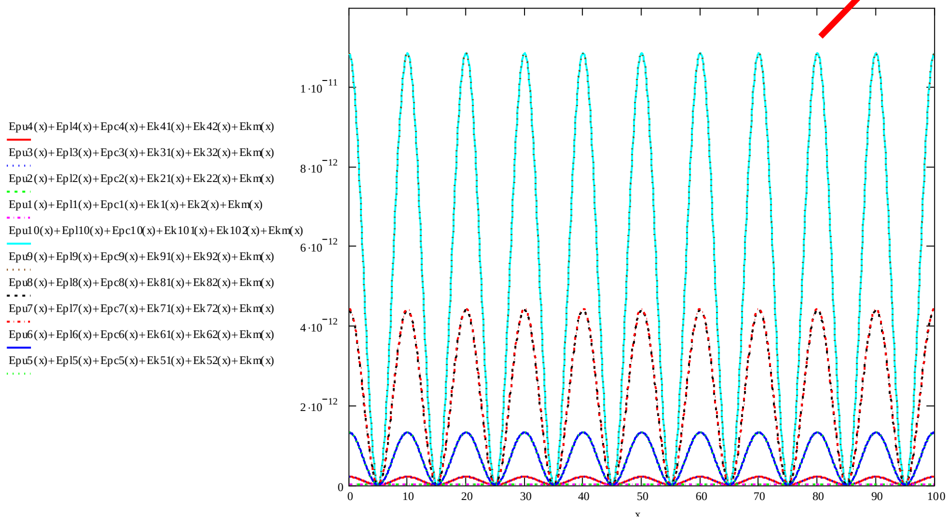

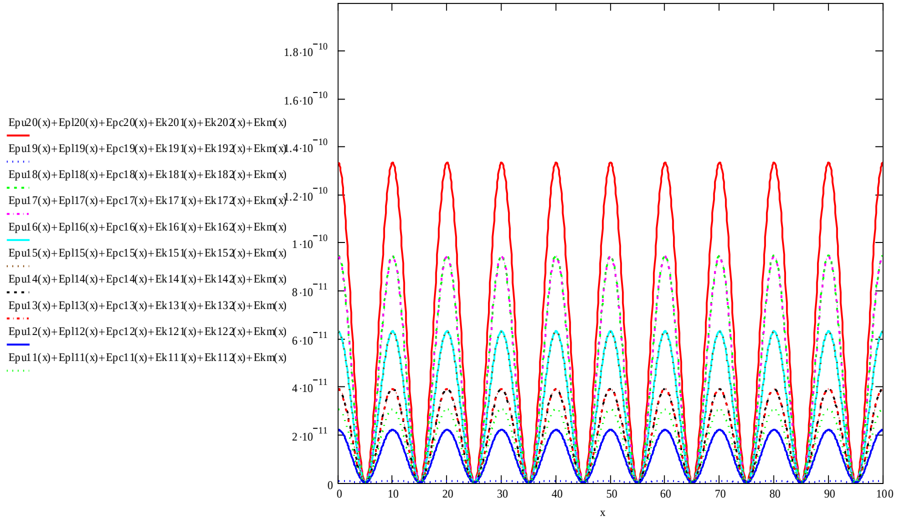

Results

Total mechanical energy of 10 pairs of homologue chromosomes in the system of mitotic spindle

Case

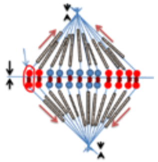

Same frequency of rheonomic centers $\Omega_1 = 0.419$ 1/s

central

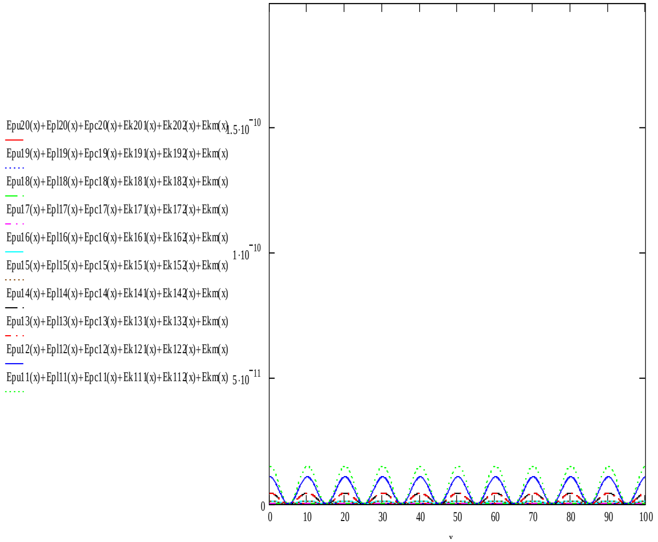

peripheral

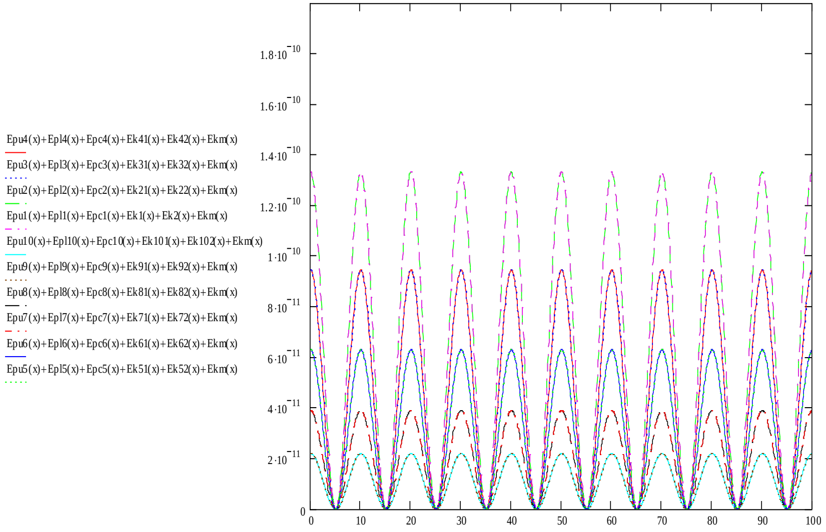

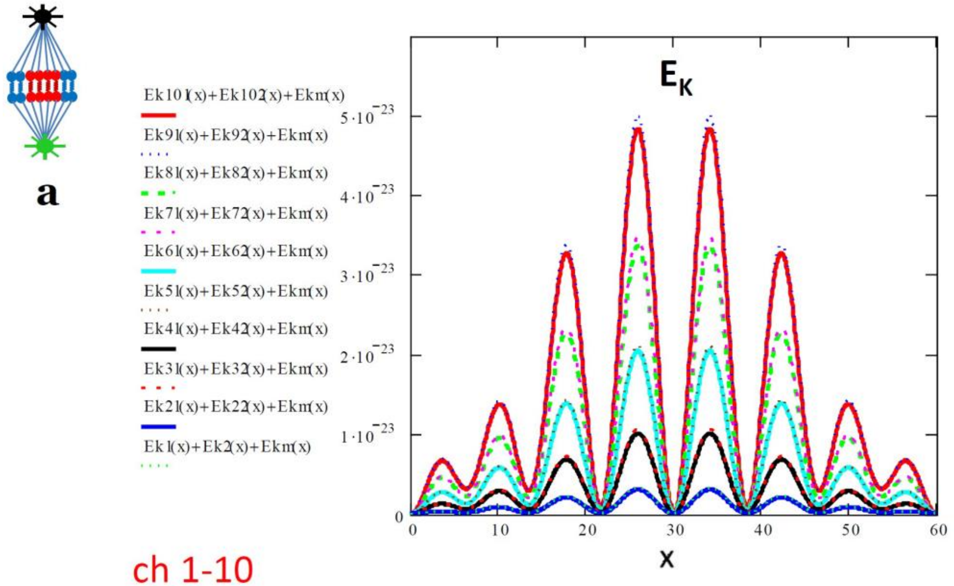

ch 1-10

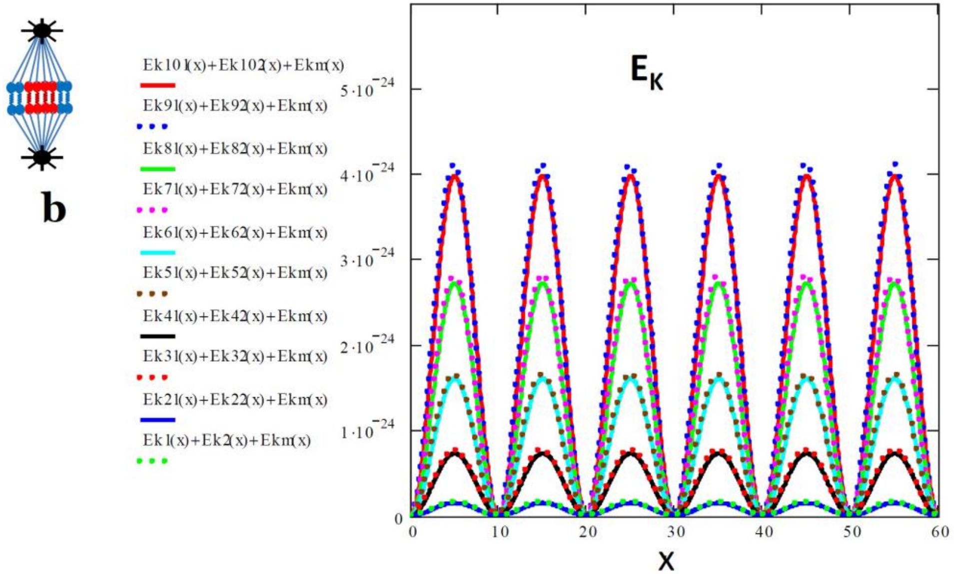

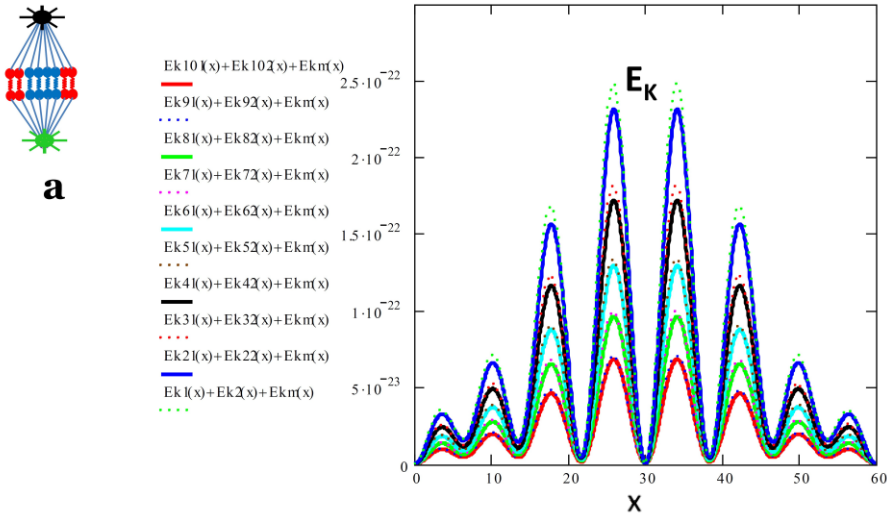

ch 1-10

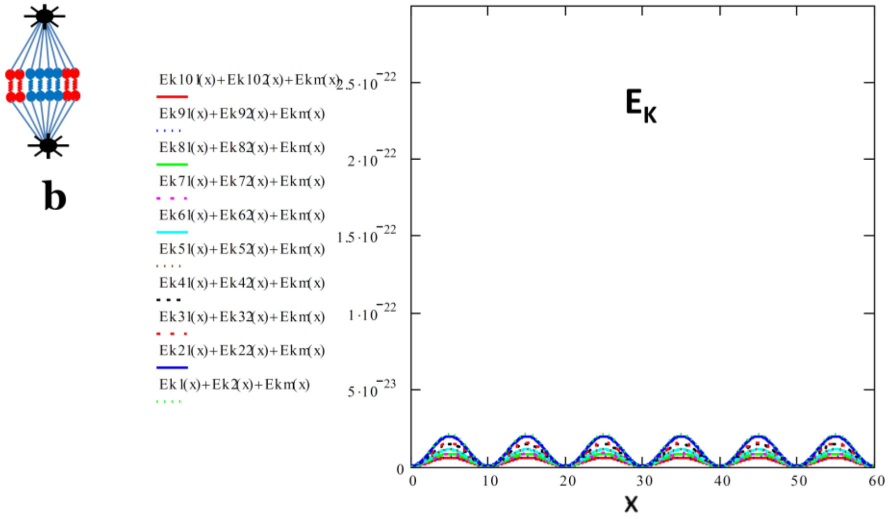

From :Hedrih, A., Hedrih, K.: Kinetic energy of dyads of sister chromatids in a biomechanical oscillatory model of the mitotic spindle. RAD Conf Proc. 3: 225–230 (2019).

- This difference in energy distribution could be of importance for the stability of the system of mitotic spindle and its energy balance.

- **Also this difference in energy distribution during metaphase may carry additional epigenetic information and could be important for process of differentiation and genesis of cancer.**

CYTOPLASM AS A VISCOUS MEDIA WITH VERY SMALL REYNOLDS NUMBERS

$$\boxed{F = \mu_d \dot{x}}$$

low Reynolds numbers

d=3 μm,
L=20 μm

ρ=1000 kg/m^3 at 37 ^{0}C

length of the cylinder

velocity

Reynolds number for a cylinder

μ=0.7 mPas

(Re=1.3·10^{-7})

u=30 nm/s

$$\boxed{\mu_d = 4\pi\mu L u \varepsilon(1 - 0.87\varepsilon^2),}$$

$$Re = \frac{\rho d u}{\mu}$$

$$\varepsilon = \left[\frac{1}{2} - \gamma - \ln\left(\frac{Re}{8}\right)\right]^{-1}$$

dynamic viscosity

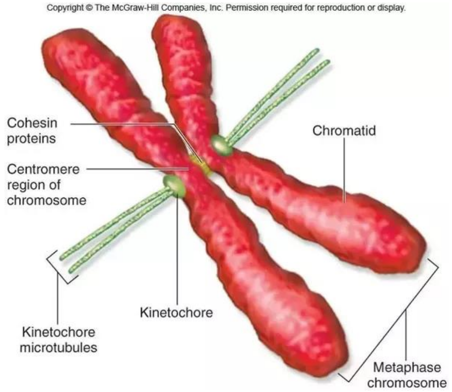

$$\boxed{\mu_d \sim 10^8}$$

$\gamma = 0.577216$ Euler's constant

FLUID RESISTANCE FORCES OF EACH SISTER CHROMATID

$$F_{w,\mathrm{u}ik} = -m_{uik}\tilde{\mu}\sqrt{\left[\left(\dot{x}_{uik} + \dot{y}_{uO1}\cos\alpha_{uik}\right)^2 + \left(\dot{y}_{uO1}\sin\alpha_{uik}\right)^2\right]}$$

$$F_{w,dik} = -m_{dik}\tilde{\mu}\sqrt{\left[\left(\dot{x}_{dik} + \dot{y}_{dO2}\cos\alpha_{dik}\right)^2 + \left(\dot{y}_{dO2}\sin\alpha_{dik}\right)^2\right]}$$

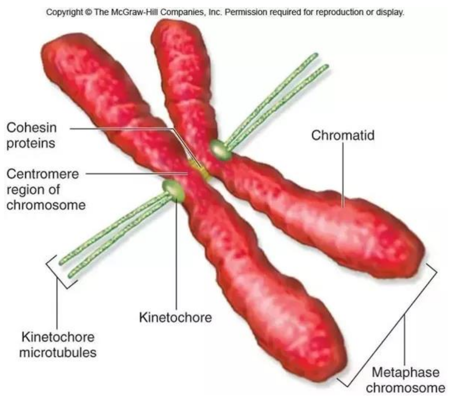

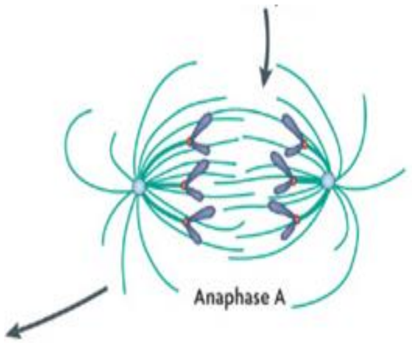

ENERGY OF MOVING HROMATIDES

$$E_{T,ik} = E_{k,ik} + E_{p,ip}$$

$$E_p = \frac{1}{2} c_{uik} x^2_{uik} + \frac{1}{2} c_{dik} x^2_{dik} + \frac{1}{2} c_{ik} [(y_{uO1} + y_{dO1}) + (x_{uik} \sin \alpha_{uik} + x_{dik} \sin \alpha_{dik})]^2$$

$$\mathbf{E}_{K,ik} = \frac{1}{2} m_{uik} \left[(\dot{x}_{uik} + \dot{y}_{uO1} \cos \alpha_{uik})^2 + (\dot{y}_{uO1} \sin \alpha_{uik})^2 \right] + \frac{1}{2} M_u (\dot{y}_{uO1})^2 + $$
$$+ \frac{1}{2} m_{dik} \left[(\dot{x}_{dik} + \dot{y}_{dO2} \cos \alpha_{dik})^2 + (\dot{y}_{dO2} \sin \alpha_{dik})^2 \right] + \frac{1}{2} M_d (\dot{y}_{dO2})^2$$

$$i = 1, 2 \ldots 20$$

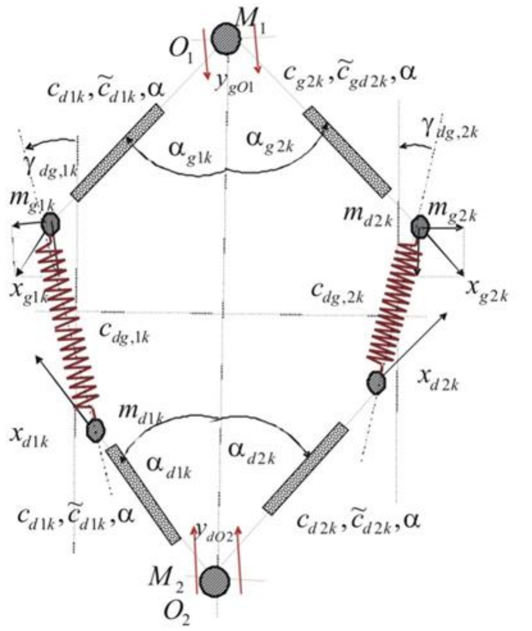

$$\Phi_{ik} = \frac{1}{2} m_{gik} \mu \dot{x}^2_{gik} + \frac{1}{2} m_{dik} \mu \dot{x}^2_{dik} + \frac{1}{2} M_g \mu (\dot{y}_{gO1})^2 + \frac{1}{2} M_d \mu (\dot{y}_{dO1})^2$$

Rayleigh function of energy dissipation

RAYLEIGH FUNCTION OF ENERGY DISSIPATION

$$\frac{d\left(\mathbf{E}_{K,ik}+\mathbf{E}_{P,ik}\right)}{dt}=-2\Phi_{ik}$$

System is non-conservative

$$\Phi_{ik}=\frac{1}{2}m_{gik}\mu\left[\left(\dot{x}_{uik}+\dot{y}_{uO1}\cos\alpha_{uik}\right)^2+\left(\dot{y}_{uO1}\sin\alpha_{uik}\right)^2\right]+\frac{1}{2}M_g\mu\left(\dot{y}_{gO1}\right)+$$

$$+\frac{1}{2}m_{dik}\mu\left[\left(\dot{x}_{dik}+\dot{y}_{dO2}\cos\alpha_{dik}\right)^2+\left(\dot{y}_{dO2}\sin\alpha_{dik}\right)^2\right]+\frac{1}{2}M_d\mu\left(\dot{y}_{dO1}\right)^2$$

Some conclusions

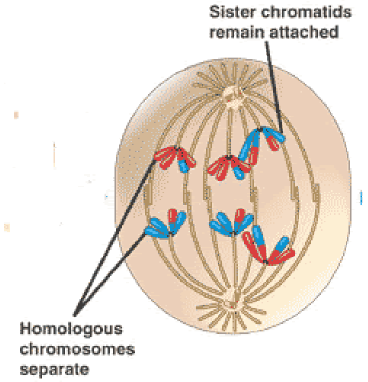

- The Rayleigh function of energy dissipation is used to model oscillatory behaviour of moving sister chromatids in anaphase of mitosis
- Using the presented methodology, it is possible to numerically solve the cases when the sister chromatids are still connected, but also the case when their final separation occurs during anaphase II.
- In that case, each sister chromatid bound to the rheonomic center represents an oscillator with one degree of freedom of movement.
- we are free to suggest that chromosomes and sister chromatids use relaxation oscillations as a possible mechanism of movements through the cytoplasm as a viscous fluid.
- It is also possible that citoplasm is acting as a fluid that passes through a sol-gel transition phase during mitosis, and that this transition can have different speeds.

Thank you for your attention!

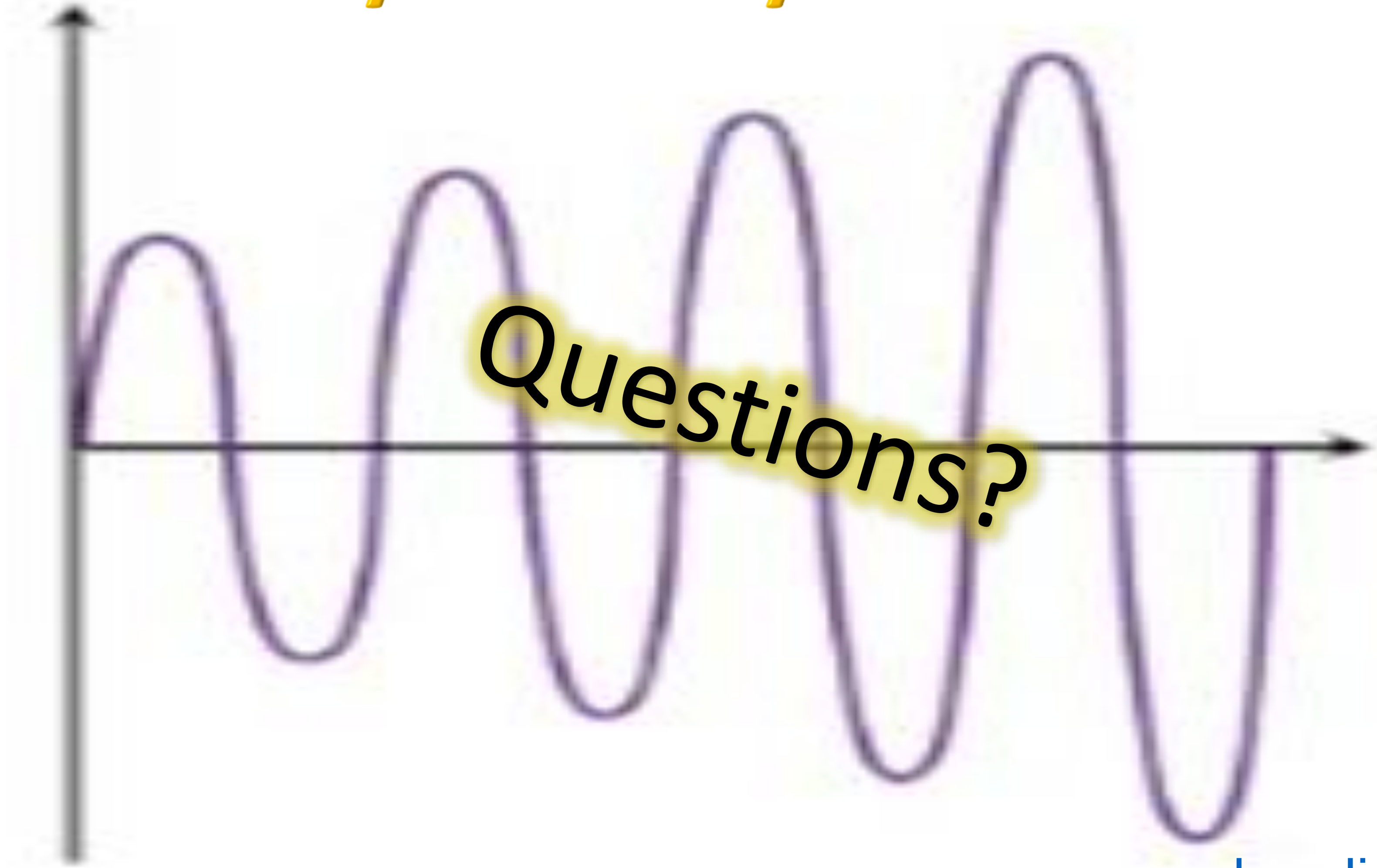

handjeka@gmail.com